# A project report on

## NUMERICAL STUDY OF AXIAL WALL CONDUCTION IN PARTIALLY HEATED MICROTUBES

**By**

**MOTISH KUMAR**

**ROLL NO: 211ME3185**

## Under the guidance of

**Dr. MANOJ K. MOHARANA**


**Department of Mechanical Engineering**

**National Institute of Technology Rourkela**

**Rourkela, 2013**

# National Institute of Technology
# Rourkela

## CERTIFICATE

This is to certify that the thesis entitled, **"NUMERICAL STUDY OF AXIAL WALL CONDUCTION IN PARTIALLY HEATED MICROTUBES"** submitted by **Mr. Motish Kumar** in partial fulfillment of the requirements for the award of Master of Technology Degree in **Mechanical Engineering** with specialization in **Thermal Engineering** at the National Institute of Technology, Rourkela (Deemed University) is an authentic work carried out by him under my supervision and guidance.

To the best of my knowledge, the matter embodied in the thesis has not been submitted to any other University/ Institute for the award of any degree or diploma.

**Date:**

**Dr. Manoj Kumar Moharana**
**Department of Mechanical Engineering**
**National Institute of Technology Rourkela**
**Rourkela– 769008**

# ACKNOWLEDGEMENT

I would like to thank and express my gratitude towards my supervisor **Dr. Manoj K Moharana** for his extensive support throughout this project work. I am greatly indebted to him for giving me the opportunity to work with him and for his belief in me during the hard time in the course of this work. His valuable suggestions and constant encouragement helped me to complete the project work successfully. Working under him has indeed been a great experience and inspiration for me.

I would also like to thank **Mechanical Department** specially **Dr. A.K Satapathy** who has provided the **CFD Lab** Where I completed the maximum part of my project work.

**Date:**

**Place:** **Motish kumar**

# ABSTRACT

A numerical analysis has been carried out for internal convective flows in a microtube subjected to conjugate heat transfer situation. This analysis has been carried out to understand the effect of axial wall conduction for simultaneously developing laminar flow and heat transfer in a circular microtube subjected to constant wall temperature boundary condition imposed on its outer surface. Practically in many a situations the two ends or one of the ends of the microtube are insulated because of demand of physical situation. In this background, we have considered for four most practical cases of partial heating of microtubes: (i) the outer surface of the microtube is subjected to constant wall temperature over its full length (ii) 10% of total length at both the inlet and the outlet end are insulated while the remaining length is subjected to constant wall temperature boundary condition (iii) 10% of total length at inlet is insulated while the remaining length is subjected to constant wall temperature boundary condition (iv) 10% of total length at outlet is insulated while the remaining length is subjected to constant wall temperature boundary condition. Simulations have been carried out for a wide range of pipe wall to fluid conductivity ratio ($k_{sf}$: 2 - 646), pipe wall thickness to inner radius ratio ($\delta_{sf}$:1, 10), and flow Re (100 - 500). These parametric variations cover the typical range of applications encountered in microfluids/microscale heat transfer domains. For partial heated microtube it is found that the average Nusselt number ($Nu_{avg}$) is increasing with decreasing $k_{sf}$. At very low $k_{sf}$ it is found that for smaller $\delta_{sf}$, ($Nu_{avg}$) again starts decreasing, but at higher $k_{sf}$ it continues to increase. This is due to absence of axial wall conduction and lower total heating length. But at higher $k_{sf}$ the effective heating length increases due to axial wall conduction. Overall, at higher $\delta_{sf}$, the trend is same as full heating case because of axial wall conduction at both the inlet and the outlet ends due to thick solid wall.

**Keywords:** Microtube, Axial conduction, Partial heating, Laminar flow, Constant wall temperature.

# Contents

# List of figure

# List of Table

## Nomenclature

| | |
|---|---|
| $T_w$ | Wall temperature, K |
| $T_f$ | Bulk fluid Temperature, K |
| $q_w$ | Wall heat flux, $W/m^2$ |
| $\bar{u}$ | Average velocity at inlet, m/s |
| $k_s$ | Solid thermal conductivity, W/mK |
| $k_f$ | Fluid thermal conductivity, W/mK |
| $c_p$ | Specific heat of fluid, J/kgK |
| $k_{sf}$ | Ratio of $k_s$ and $k_f$ |
| L | Total length of tube, m |
| P | Parameter for axial conduction |
| $D_i$ | Inner diameter of microtube, m |
| $r_i$ | Inner radius of microtube, m |
| $h_z$ | Local heat transfer coefficient, $W/m^2K$ |
| $Nu_z$ | Local nusselt number |
| $Nu_{fd}$ | Nusselt number for fully developed flow |
| $\overline{Nu}$ | Average nusselt number |
| Pr | Prandtl number |
| Re | Reynolds number |
| Pe | Peclet number |
| u | Velocity in the axial direction, m/s |
| $q''$ | Heat flux experienced at the solid-fluid interface of the microtube, $W/m^2$ |
| $q''_w$ | Heat flux experienced on the outer surface of the microtube, $W/m^2$ |
| Z | Axial coordinate, m |
| $Z^*$ | Non dimensional axial coordinate |

**Greek symbols**

| | |
|---|---|
| $\delta_f$ | Inner radius of the tube, m |
| $\delta_s$ | Thickness of the tube wall, m |
| $\delta_{sf}$ | Ratio of $\delta_s$ and $\delta_f$ (-) |
| $\nabla$ | Differential parameter |

μ Dynamic viscosity, Pa-s

ρ Density, $kg/m^3$

Φ Non-dimensional local heat flux (-)

Θ Non-dimensional temperature (-)

**Subscripts**

f Fluid

i Inner surface of tube

o Outer surface of tube

s Solid

w Outer wall surface of tube

# Chapter 1

## Introduction

The recent developments in electronics devices has led to increasing processor speed, that comes with increased heat generation and decreased processor size; thus doubling the heat density. Moore's law states that "the semiconductor transistor density and hence the performance doubles roughly in every 18 months" (Moore, 1965). Thus, thermal management of electronic devices is gaining importance day by day.

Tuckerman and Pease (1981) had demonstrated that microchannels are capable of removing high heat flux; therefore ideal for cooling electronics chips. Conventionally, heat transfer is directly proportional to the surface area of heat transfer and the temperature difference. While temperature difference is restricted by the application, the surface area per unit volume controls the heat transfer. Owing to its higher surface area per unit volume compared to a conventional size channel, microchannels provide higher heat removal rate. With advances in microfabrication techniques, microchannels of different shapes and size can be fabricated easily, thus gaining momentum in their use for a wide variety of engineering applications.

The developments in micro-manufacturing technology and the inspiring work by Tuckerman and Pease (1981) led to widespread use of microchannel heat exchangers for electronics cooling,

micro reaction, space craft thermal management etc. to mention a few. The early developments during the first 10-20 years in the field of microchannel heat transfer with historical perspective are available in Goodling (1993) and Mehendale et al. (2000). With growing literature in this field, few books/monograms dedicated to microchannel fluid flow and heat transfer have been published (Kakac et al., 2005; Kandlikar et al. 2006; Yarin et al., 2009). Scaling effects play a vital role in microscale single-phase fluid flow and heat transfer devices (Morini, 2006; Rosa et al., 2009). Among different scaling effects that play some role at microscale, axial back conduction play very critical role in the performance of a microscale heat exchanger device. In this background the present work is focused on the role of axial back conduction in microtubes and provides (i) an exhaustive in-depth review of research works done so far (ii) numerical study of axial wall conduction in partially heated microtubes.

### 1.1. What is axial back conduction?

Consider laminar fluid flow through a circular duct subjected to "constant heat flux" boundary condition on its outer surface. In this condition it is considered that the heat applied on the outer surface flows in radial direction along the solid wall of the duct by means of conduction. Once it reaches the solid-fluid interface, the heat flows into water and gets carried along with the flow of the fluid. The surface area (solid-fluid interface) increases linearly in the flow direction. So, heat is added to fluid continuously as the fluid moves in the diction of flow, thus bulk fluid temperature increases in a linear manner. The duct wall (at the solid-fluid interface) temperature also increases linearly beyond the thermally developing zone. The applied heat flux (which is uniformly applied over the outer surface of the duct) is given by:

$$q'' = h \cdot (T_w - T_f) \tag{1.1}$$

The duct wall temperature can be calculated from the above heat balance equation:

$$T_w = \frac{q''}{h} + T_f \qquad (1.2)$$

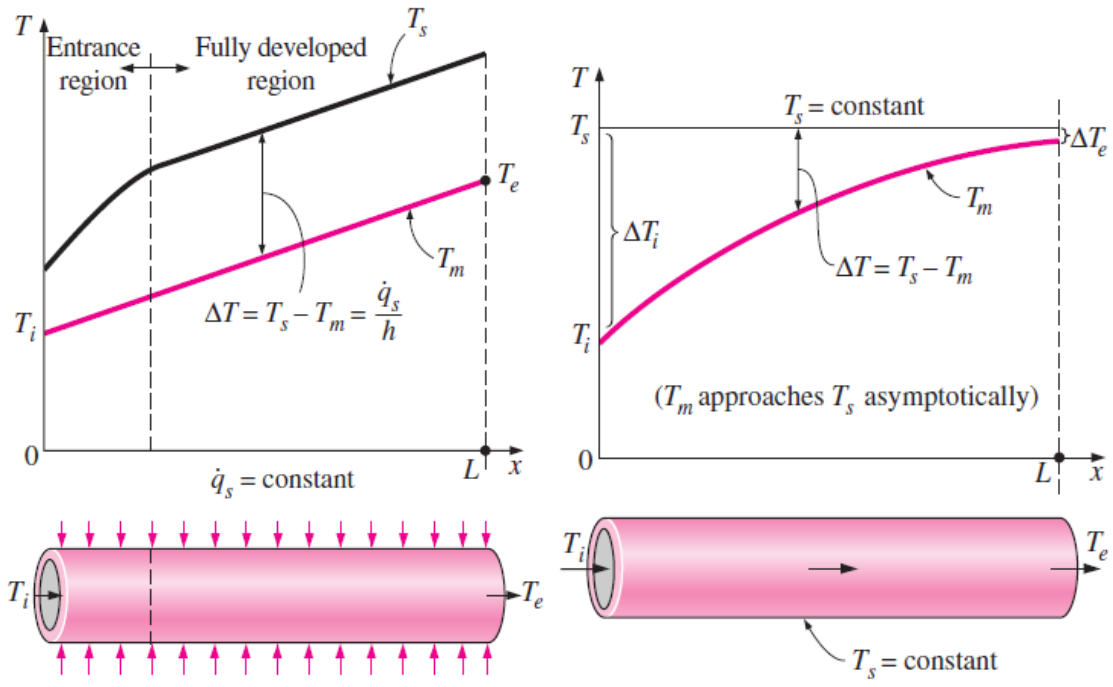


Fig. 1.1: Variation of bulk fluid and local wall temperature in the flow direction of a circular duct subjected to (a) constant wall heat flux (b) constant wall temperature (Cengel, 2003).

In the fully developed region, the wall temperature will also increase linearly in the direction of flow as the heat transfer coefficient h is constant in this region. This analysis is based on the assumption that the fluid properties remain constant during flow through the duct. The typical representation of such phenomena is shown in Fig. 1.1(a) where the bulk fluid temperature and duct wall temperature at the solid-fluid interface is varying in the axial direction. Fig. 1.1(b) shows the similar representation when the outer surface is maintained at constant uniform temperature, called constant wall temperature boundary condition. In this case the axial variation

of bulk fluid temperature is nonlinear, and it approaches asymptotically equal to wall temperature far away from the inlet.

Here it is to mention that the constant heat flux/constant wall temperature is applied on the outer surface of the circular duct and the duct wall temperature used in Eq. (1.1) or (1.2) indicate the temperature of the inner surface of the duct i.e. the temperature of the solid-fluid interface. It is to note that the duct wall is finite in thickness. Therefore when the heat flux is applied on the outer surface, it gets conducted radially towards the center of the tube. Once the heat reaches the inner surface of the tube, it is carried by the working fluid in the direction of flow.

From Fig. 1.1 (a), it can be observed that there is a temperature difference between any two points along the axial direction (both in the solid and the fluid medium) and the maximum temperature difference between the inlet and the outlet of the heated duct. This axial temperature difference causes potential for heat conduction axially along the solid, and also along the fluid towards inlet of the tube i.e. in a direction opposite to the direction of fluid flow. Such a situation is called "*axial back conduction*" and leads to conjugate heat transfer. It is interesting to observe in Fig. 1.1(b) that there is no axial temperature gradient when constant wall temperature boundary condition is applied. As of now it is expected that under such condition there will not be any axial heat conduction, but needs to confirm this from the present work.

### 1.2. Difference between conventional size and micro size channels:

There is some basic difference between conventional size and micro size channels. Consider the case of circular ducts. In conventional size heat exchangers, the duct wall thickness

is very less compared to the inner diameter. But for flow in microchannels the solid wall thickness is normally of the same order or larger than the channel diameter. Figure 1.2 shows cross-sectional views of a microtube used in experimental investigations. In Fig. 1.2, it can be observed that the wall thickness is comparatively high than conventional circular ducts. Secondly, it can also be observed that with decreasing inner diameter of the tube, the relative wall thickness is increasing.

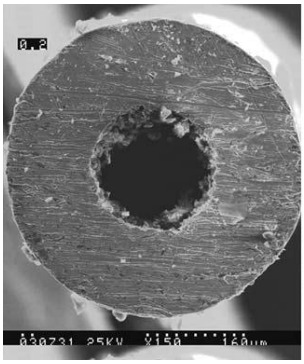

Fig. 1.2: Cross-sectional view of microtubes (Liu et al. 2007)

In the context of laminar duct flow in microchannels, conjugate heat transfer leads to a strong multidimensional coupling. The small dimensions of microchannels in the transverse direction are often comparable to the substrate thickness. As the hydraulic diameter of microchannels decreases, this coupling between the substrate and bulk fluid temperatures becomes significant. It is important to explicitly identify the thermofluidic parameters of interest which lead to a distortion in the boundary conditions and thus the true estimation of species transfer coefficients.

In this background a numerical simulation is undertaken to study axial wall conduction in partially heated microtubes subjected to constant wall temperature on the outer surface of the heated portion. A wide parametric variation of thermal conductivity, wall thickness and flow Re

are considered for a detailed investigation which is described in chapter 3. Before we could start the numerical simulation, chapter 2 describes a detailed review of literature on axial wall conduction in microchannels.

# Chapter 2

## Literature review

Axial back conduction is not a new concept, rather a well-established concept by now. Secondly this concept is not limited to microchannels only. A detailed review on early developments on axial wall conduction in conventional size heat exchangers was presented by Peterson (1999). Many studies do exist in open literature that deal with axial wall conduction in conventional size channels (Bahnke and Howard, 1964; Petukhov, 1967; Mori et al., 1974; Barozzi G.S., Pagliarini, 1985; Chiou, 1980; Faghri and Sparrow, 1980; Cotton and Jackson, 1985).

Davis and Gill (1970), Mori et al. (1979) have studied the effect of axial conduction in the wall of a microchannel. They found that the value of Pe is high correspondingly.so axial conduction in the fluid can be neglected.

Cotton and Jackson (1985) have related the effect of axial back conduction with following parameter which is

$$P = \frac{k_s}{k_f}\left[\frac{\delta}{D_i}\left(1+\frac{\delta}{D_i}\right)\right]\frac{1}{Pe^2} \qquad (2.1)$$

Where P is parameter for axial conduction.

Kim and Kim (1999) have studied the effect of axial conduction at the wall for the micro-channel heat sinks for both circular and rectangular channel geometries.

Qu et al. (2000) have analyzed the heat transfer for water flow in trapezoidal silicon microchannels with a hydraulic diameter ranging from 62 to 169 mm. They conducted both experiment as well as numerical analysis. Numerical analysis was carried out by solving a conjugate heat transfer problem involving simultaneous determination of the temperature field in both the solid and the fluid regions.

The heat transfer and fluid flow phenomena have been investigated by Toh et al. (2002) inside a three dimensional heated microchannel. They solved steady, laminar flow and heat transfer equations using a finite-volume method. The numerical procedure is validated with available experimental data. They found that at lower Reynolds numbers the temperature of the water increases, leading to a decrease in the viscosity and hence smaller frictional losses.

Maranzana et al. (2004) carried out analytical study as well as numerical simulation to understand axial heat conduction phenomena in a mini/micro counter flow heat exchanger. Based on their analysis, they stated that the effect of axial conduction in the substrate on the heat transfer coefficient can be neglected if $M<10^{-2}$. Both the conduction parameter (k) and the axial conduction number (M) are based on the assumption that the axial temperature difference between the inlet and outlet location in the solid substrate ($\Delta T_s$) as well as in fluid ($\Delta T_f$) domain is same; this assumption is rather unrealistic though.

Tiselj et al. (2004) carried both experiment and numerical analysis to evaluate heat transfer characteristics of water flowing through triangular silicon micro-channels with hydraulic diameter of 160 μm in the range of Reynolds number Re = 3.2–64. As It was shown that the bulk water temperature, as well as the wall temperature of the heated wall, does not vary linearly in

the direction of channel. The experimental results and numerical predictions are very much similar. Both the water and heated surface temperatures do not change monotonously. At some values of z the temperature gradients change sign. This value depends on the Reynolds number and shifts to the channel outlet with an increase in Re. This trend was observed for all flow and heat flux conditions of the present study.

Gamrat et al. (2005) carried out the numerical analysis for convective heat transfer both two and three dimension rectangular micro pipe to know about the conduction and entrance effect. Comparison between numerical and experimental results for two channel spacing the wall temperature is slightly underestimated by the numerical model Nu is slightly overestimated (about 10–20%) by the numerical model. Numerical simulations show that there is no size effect on heat transfer when the channel spacing is reduced from 1 mm down to 0.1 mm. Hetsroni et al. (2005) had made some setup and done the experimental analysis with micro pipe and got some result that The inner diameters of smooth micro-tubes were 125.4, 300, and 500 lm and the flow regime was laminar with Reynolds number Re = 95–774. The micro-tube was placed inside a vacuum chamber to eliminate heat loss to the ambient and constant temperature is maintained at outer wall. Then it has been observed that for both condition i.e constant wall heat flux and constant wall temperature the value of Nusselt number is very nearer to numerical analysis result.

Celata et al. (2006) experimentally investigated single-phase laminar flow in circular micro-ducts of diameter 528, 325, 259 and 120mm. Results was clearly showing that the decrease of Nusselt number with decreasing diameter. An axial dependence that is linked to thermal entrance effects and a dependence of the Nusselt number also on Reynolds number is found. Investigation

was also done for the possible occurrence of scaling effects such as axial conduction in the wall of mico-duct, viscous heating of fluid and thermal entrance length effects.

Lelea (2007) He was the first who simulated the partially heated heat transfer problem. He investigated for the conjugate heat transfer of the water flow inside the microtube of different dimensions, $D_i/D_o$ = 0.1/03 and 0.1/0.5 mm. The Re value up to 200, and input heat transfer rate of $Q_0$ = 0.1 W is considered. Lelea (2007) studied Two different cases of the partial heating applied at outside of the tube wall, when the tube wall was heated near the inlet of the tube (upstream heating) and when the outlet portion of the wall was heated (downstream heating). He observed effect of axial conduction in the case of partial heating. After the numerical analysis with considering the heat losses defined by the heat transfer rate ratio $Q/Q_0$,Influence of the heating position, tube material, wall thickness and Re some result has been outlined. Wall axial conduction has almost negligible influence on thermal characteristics of the stainless steel tubes, irrespective of the heating position, wall thickness or Re. For the case of upstream heating, the heat is dispersed through the tube wall in the upstream section of the fluid flow. There is an abrupt decreasing of the local Nu at the end of the heating section, but the local Nu in the fully developed region has the usual value Nu= 4.36 for constant heat flux applied at solid-fluid interface when there is no wall thickness.

Yang and Lin (2007) experimentally investigated heat transfer performance of water flowing through microtubes (D = 123 to 962 mm) using non-intrusive liquid crystal thermography. This investigation concluded that transition occurs at Re values 2300 to 3000.

García et al. (2009) studied experimentally the single phase thermo-hydrodynamic performance of two square microchannel (100 and 200mm respectively) with using deionized water. Experimental result showed that for both for pressure drop and heat transfer, and for a

wide range of Reynolds numbers (except for very low Re), are very similar with the conventional theory; no special effects related to the small dimension of the channels were observed. Conventional theory held good for fully-developed laminar and turbulent flow and heat transfer performance. Also, no significant size effect was observed for the range of diameters used. It was studied that the discrepancy in the Nusselt number for developing flows was increasing with decreasing diameter.

Hernando et al. (2009) these people were presented an experimental setup for an experimental analysis of the hydrodynamic and thermal performance of micro-heat exchangers. The fluid used was deionized water and there is always single phase flow along the fluid circuit. Fluid pressure drop along the heat exchanger and the heat transfer were measured. Result show that the experimental results fit with these theories. There are no effects of heat transfer enhancement or pressure drop increase was observed as a consequence of the small scale of the microchannels.

Lelea (2009) analyzed the influence of the heating position on the thermal and hydrodynamic behavior. The laminar fluid flow and the water as a working fluid are considered. Observation has been made that partial heating together with variable viscosity has a strong influence on thermal and hydrodynamic characteristics of the micro-heat sink. And the heating position influences both of the hydrodynamic and thermal characteristics of a micro-heat sink.

Satapathy (2010) solved the steady study heat transfer for laminar two dimensional and rarefied gas flows in an infinite microtube subjected to mix boundary condition analytically. In this paper he mainly focused on velocity slip and temperature jump boundary condition on the wall.The energy equation is solved analytically by separation of variable method.For the hot fluid and cold wall situation the local bulk mean temperature increases with increase in peclet number but decreases with increase in knudsen number. Therrmal entrance length increases as

peclet number or knudsen number. Local Nusselt number increases with increase in Peclet number but decrease with increase in knudsen number.

Zhang et al. (2010) The effects of wall axial heat conduction in a conjugate heat transfer problem in simultaneously developing laminar flow and heat transfer in straight thick wall of circular tube with constant outside wall temperature are numerically investigated by them. He used the finite-volume-method to to discretize the governing equations; the SGSD scheme is used for the discretization of the convective term, and the SIMPLEC algorithm. And plotted the local Nusselt number, wall and fluid temperature corresponding to axial location to study the effect of axial wall conduction effect.

An analysis is done by Cole and Cetin (2011) for conjugate heat transfer in a parallel-plate microchannel. Axial conduction in both fluid and in the adjacent wall are included. Fluid has constant property with a fully-developed velocity distribution inside the microchannel. The microchannel is heated by a uniform heat flux boundary condition applied to the outside of the channel wall.

Moharana et al. (2011) had both experimentaily and numerically analysis axial wall conduction in single-phase simultaneously developing flow in a rectangular mini-channel array. They found that at higher value of the axial conduction number (M), the experimental setup is prone to conjugate effects as a consequence of axial back conduction in the substrate. This causes the local experimental Nusselt numbers to be smaller than the actual counterparts predicted by numerical the model

Moharana et al. (2012) numerically studied axial wall conduction in a square microchannel carved on a solid substrate and considered wide parametric variation of conductivity ratio, substrate thickness and flow Re. The bottom wall of the solid substrate was subjected to constant

heat flux boundary condition and all the remaining walls of the substrate exposed to the surroundings were kept adiabatic. Moharana et al. (2012)

They got some different variation which is as follows , for a given flow rate and $\delta_{sf}$, the thermal conductivity ratio $k_{sf}$ is the key factor in determining the effects of axial wall conduction on the heat transport behavior. Higher $k_{sf}$ leads to axial back conduction, thus decreasing the value of average Nusselt number as compared to the value of Nusselt number obtained for the case when the wall thickness is negligible. Very low $k_{sf}$ leads to a situation where the channel heat transfer can be compared to a channel having zero wall thickness with only one side heated with a constant heat flux and the rest of the three sides being adiabatic; this leads to lower average Nusselt number. The results explicitly indicate the existence of an optimum value of the thermal conductivity ratio for maximizing the average Nusselt number, for a given flow rate and wall thickness ratio. It has also been shown that similar phenomena will be observed in substrates having a tubular geometry.

Moharana et al. (2012) studied the effect of axial conduction in a microtube for wide range of Re, ratio of wall thickness to inner diameter and thermal conductivity ratio. A two dimensional numerical simulation has been carried out for both, constant wall heat flux and constant wall temperature, at the outer surface of the tube, while flow of fluid through the microtube is laminar, simultaneously developing in nature. After the simulation it has been shown that $k_{sf}$ plays a dominant role in the conjugate heat transfer process. When the constant heat flux boundary condition is applied on the outer surface of the microtube, there exists an optimum value of $k_{sf}$ for which the average Nusselt number ($Nu_{avg.}$) over the microtube length is maximum. However, when constant wall temperature is applied on the outer surface of the

microtube, no such optimum $k_{sf}$ value is observed at which $Nu_{avg.}$ is maximum. The value of $Nu_{avg.}$is found to be increasing with decreasing value $k_{sf}$.

Rahimi and Mehryar (2012) had studied the axial heat conduction effect on the local Nusselt number.at the entrance and ending region of circular micro pipe. He proposed the result for constant heat flux boundary condition.

"Entrance local Nusselt number" In this section, the effects of solid wall to fluid thermal conductivity ratio and outside to inside diameter ratio on the local Nusselt number at the entrance region of the micro pipes are investigated. It should be noted that as the axial heat conduction in the wall is proportional to the wall thermal conductivity and normal surface area, so the wall thickness has more or less the same effect as wall thermal conductivity on the local heat transfer coefficient. So increase of the ratio $D_o/D_i$ increases the inside wall heat flux at the entrance region and the Nusselt number is reduced.

"Ending region" local Nusselt number besides the entrance and fully developed regions there is an ending region where local Nusselt number considerably deviates from fully developed value. The ending length and the deviation from fully developed Nusselt number increase with increasing the axial heat conduction in the wall. The reason of this phenomenon can be explained by figure, an axisymmetric micro pipe with the effect of wall axial heat conduction has been schematically shown where a constant heat flow rate per unit length is imposed on the outside surface of the duct wall. The high heat flux at the entrance causes a reduction in heat flux at the ending region because the total heat on the inside and outside wall should be the same. Results showed that the axial heat conduction in the duct wall due to wall thermal conductivity and its thickness causes a reduction in the local Nusselt number at the entrance region and also a deviation in the local Nusselt number at the ending region of the micro pipe.

For a three dimensional rectangular shaped microchannel numerical simulation has been carried out by Moharana et al, (2012). In this analysis a substrate of fixed size (0.6 mm × 0.4 mm × 60 mm) is selected and the channel width and height were varied independently such that the microchannel aspect ratio varies from 1.0 to 4.0. And Moharana et al, (2012) found the effect of microchannel aspect ratio on axial back conduction. The Constant heat flux boundary condition was applied at the bottom of the substrate while all its other surfaces were kept insulated. After the simulation it has been found that the average Nusselt number is minimum corresponding to channel aspect ratio of 2.0, irrespective of the conductivity ratio of the solid substrate and the working fluid.

Although a number of numerical and experimental studies have been performed on the effect of wall heat conduction on hydro-dynamically and/or thermally developing flows in mini/microchannels, an explicit discerning parameter for judging the effect of axial conduction in the substrate on the local and average Nusselt number in the entry length is not available especially for partial heating case. Sufficient number of parametric studies is also not readily available. In practical applications, the heating length is not always equal to the total length of the microchannels. In most of the existing studies (except Lelea (2007, 2009)) the heating length was same as the total length of the microchanel.

In this background, a two-dimensional numerical study has been undertaken to study the effects of axial wall conduction in a conjugate heat transfer situation in simultaneously developing laminar flow and heat transfer in a partially heated microtube subjected to constant wall temperature boundary condition on its outer surface. The detailed numerical procedure adopted is presented in next chapter.

# Chapter 3

## Numerical Simulation

### 3.1 Introduction

In this work a two-dimensional numerical study has been undertaken to study the effects of axial wall conduction in conjugate heat transfer situation in simultaneously developing laminar flow and heat transfer in a partially heated microtube subjected to constant wall temperature boundary condition on its outer surface. Normally, the inlet and outlet arrangement likely to lead partially insulated condition near the inlet and outlet of the microtube. So, a microtube of total length 60 mm is considered for the numerical study, of which 10% of its full length (i.e. 6 mm) from the inlet and the outlet in different combinations are considered to be insulated while the rest of the microtube is subjected to constant wall temperature boundary condition on its outer surface.

In this work, simultaneously developing single-phase, steady-state laminar incompressible fluid flow with constant thermo physical properties (for both solid and liquid) in microtube geometry is considered as schematically shown in Fig. 3.1. Here heat transfer through natural convection and radiation mode is neglected. The inner radius ($r_i$) of the tube is represented as $\delta_f$ and the thickness of the microtube ($r_o$ - $r_i$) is represented as $\delta_s$. Thus, a parameter called $\delta_{sf}$ is

defined as the ratio of tube thickness to the tube inner radius. The inner radius ($\delta_f$) and the length (L) of the microtube is maintained constant in the computational domain at 0.2 mm and 60 mm respectively. The microtube wall thickness ($\delta_s$) is varied such that the value of $\delta_{sf}$ = 1 and 10. Pure water (inlet temperature of 300 K, and Pr = 7) with conductivity $k_f$ is used as the working fluid. The wall conductivity ($k_s$) is varied such that $k_{sf}$ (= $k_s/k_f$) varies in the range of 2.26 – 646 (see Table 3.1). The flow Re is varied in the range of 100 – 500.

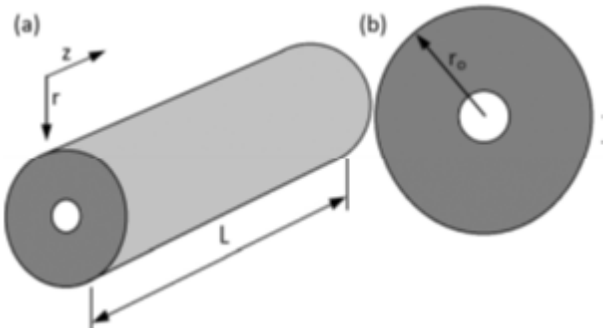

Fig. 3.1: Microtube and its cross section view

Table 3.1: Different materials used for the microtube.

| **metal** | **ρ (kg/m$^3$)** | **$C_p$ (J/kgk)** | **$K_s$ (w/mk)** | **$K_f$ (w/mk)** | **$k_{sf} = k_s/k_f$** |
|---|---|---|---|---|---|
| Silicon dioxide | 2220 | 745 | 1.38 | 0.61032 | 2.261109 |
| SS 316 | 8238 | 468 | 13.4 | 0.61032 | 21.9557 |
| Chromium steel | 7822 | 444 | 37.7 | 0.61032 | 61.77087 |
| Zink | 7140 | 389 | 116 | 0.61032 | 90.0642 |
| Alloy 195 | 2790 | 883 | 168 | 0.61032 | 275.2654 |
| aluminium | 2719 | 871 | 202.4 | 0.61032 | 337 |
| Copper | 8978 | 381 | 387.6 | 0.61032 | 646 |

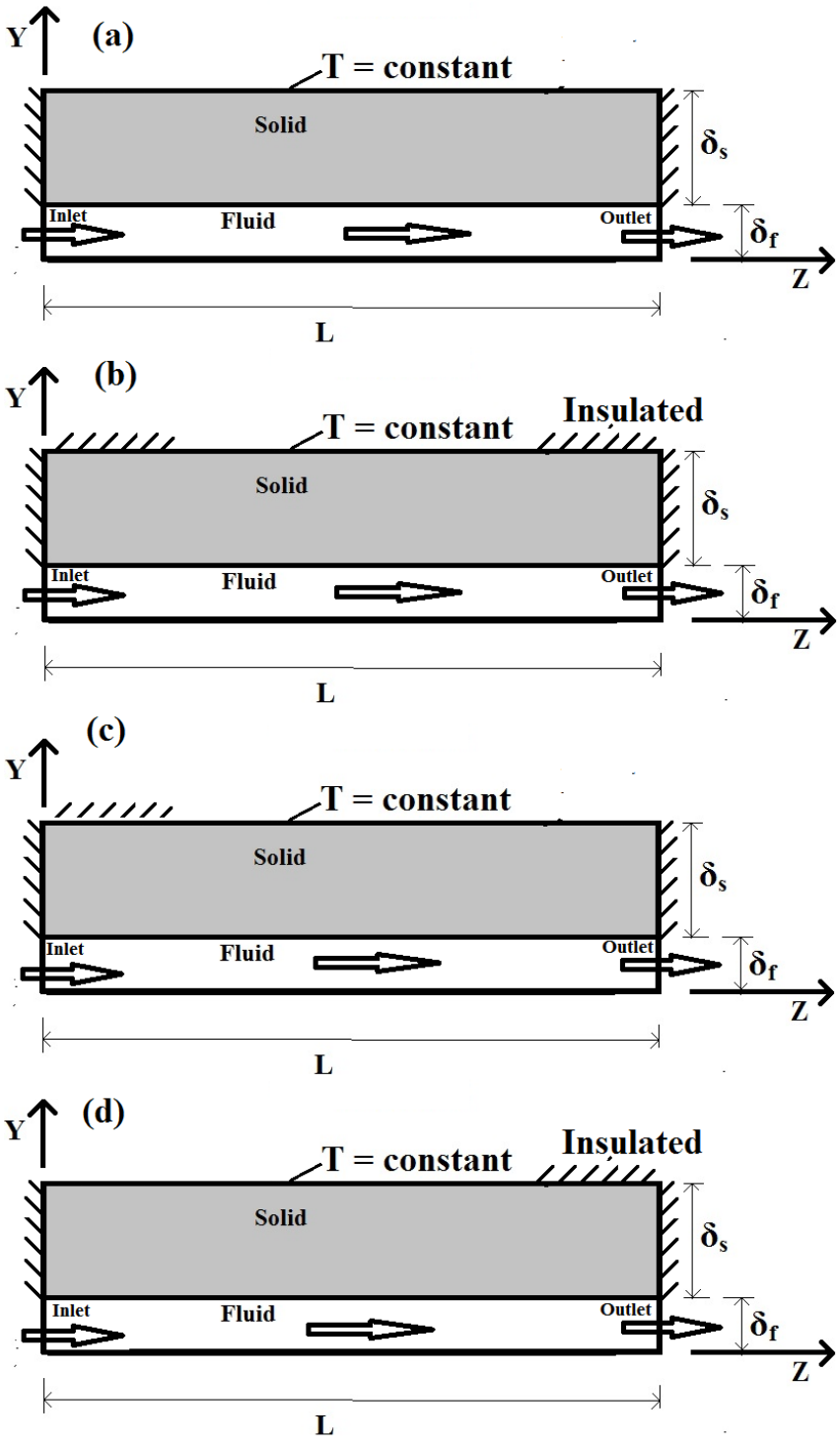


Fig. 3.2 : Four different cases of heating the microtube on its outer surface with constant wall temperature condition (a) Heating over full length of the tube (b) 6 mm insulated at each end of the tube (c) 6 mm insulated near the inlet (d) 6 mm insulated near the outlet. .

The cross-sectional solid faces of the microtube are assumed to be insulated. Considering angular symmetry, two dimensions Cartesian coordinate system (r-z) is used in our computational domain. Only one half of the transverse section of the microtube was included in the computational domain, in view of the symmetry conditions. Constant wall temperature boundary condition is applied on the outer surface of the microtube in four different ways as described below (see Fig. 3.2):

Case 1: The full length of the outer surface of the duct is subjected to constant wall temperature; see Fig. 3.2(a).

Case 2: 6 mm (10% percent of total length) each is insulated at both the inlet and the outlet end of the microtube and the outer surface of the duct is subjected to constant wall temperature in the remaining length of the tube; see Fig. 3.2(b).

Case 3: 6 mm (10% percent of total length) is insulated at the inlet end of the microtube and the outer surface of the duct is subjected to constant wall temperature in the remaining length of the tube; see Fig. 3.2(c).

Case 4: 6 mm (10% percent of total length) is insulated at the outlet end of the microtube and the outer surface of the duct is subjected to constant wall temperature in the remaining length of the tube; see Fig. 3.2(d).

The governing differential equations i.e. continuity, Navier Stokes, and Energy equations are

For fluid domain:

$$\nabla \cdot \vec{u} = 0 \tag{3.1}$$

$$\vec{u}.\nabla\vec{u} = -\frac{1}{\rho}\nabla p + \frac{\mu}{\rho}\nabla^2\vec{u} \tag{3.2}$$

$$\vec{u} \cdot \nabla T = \left(\frac{k}{\rho} \cdot C_p\right) \cdot \nabla^2 T \tag{3.3}$$

For solid domain:

$$\nabla^2 T = 0 \tag{3.4}$$

The applicable boundary conditions are as follows:

At, z = 0 to z = L and y = 0, symmetric axis

At, z = 0 and y = 0 to $y = \delta_f$, $u = \bar{u}$ (3.5)

At, z = L and y = 0 to $y = \delta_f$, gauge pressure (3.6)

At, z = 0 and $y = \delta_f$ to $y = \delta_s + \delta_f$, $\frac{\partial T}{\partial z} = 0$ (3.7)

At, z = L and $y = \delta_f$ to $y = \delta_s + \delta_f$, $\frac{\partial T}{\partial z} = 0$ (3.8)

At, z = 0 to L, $y = \delta_s + \delta_f$, Partly heating, partly insulated as described above (3.9)

The governing differential equations are solved using commercial platform Ansys-Fluent®. For pressure discretization the 'standard' scheme was used. The SIMPLE algorithm was used for velocity-pressure coupling in the multi-grid solution procedure. The momentum and energy equations were solved using 'second-order upwind'. An absolute convergence criterion for continuity and momentum equations is taken as $10^{-6}$ and for energy equation it is $10^{-9}$. Water enters the microtube with a slug velocity profile. Thus, the flow is hydro dynamically as well as thermally developing in nature at the tube inlet. The computational domain was meshed using rectangular elements and the grid independence test was ensured for every geometry included in the study.

### 3.2 Grid independence test.

In this section one sample grid independence test is presented. Similar approach adopted foe each and every geometry under consideration. For an example the local Nusselt number for flow through a circular tube subjected to constant wall temperature with zero wall thickness is presented in Fig. 3.3(a). This figure includes both developing and fully developed zone for three different mesh sizes of 3600×30, 4200×35 and 4800×40 (for half of the transverse section), for Re = 100. The local Nusselt number at the fully developed flow regime (near the tube outlet) changed by 0.7% from the mesh size of 3600×30 to 4200×35, and changed by less than 0.5% on further refinement to mesh size of 4800×40. Moving from first to the third mesh, no appreciable change is observed. So, the last grid (4800×40) was selected, It can also be observed in Fig.3.3 that the local Nusselt number values in the fully developed region is equal to the theoretical value of $Nu_T = 3.66$ where $Nu_T$ is the Nusselt number for fully developed flow in a circular tube subjected to constant wall temperature. Finer meshing was used at the boundary layer and near the inlet.

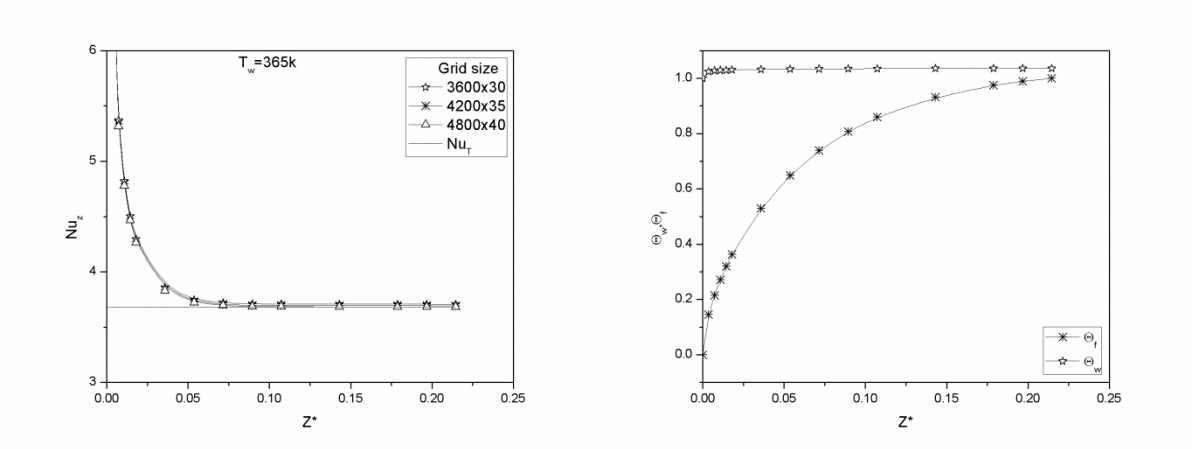


Fig. 3.3: (a) Axial variation of local Nusselt number for $\delta_s = 0$ for three different mesh sizes (b)

Corresponding axial variation of dimensionless wall and bulk fluid temperature for mesh size of $4800 \times 40$.

Figure 3.3(b) shows corresponding axial variation of dimensionless wall and bulk fluid temperature for mesh size of $4800 \times 40$. The axial variation is in line with the text book theory on internal flow through a circular tube subjected to constant wall temperature on the outer surface of the tube. Similar grid independence test are carried out and the most appropriate grid was chosen for all the geometry used in this study.

**3.3 Data reduction**

The main parameters of interest are (a) peripheral averaged local heat flux (b) local bulk fluid temperature and (c) peripheral averaged local wall temperature. These parameters allow us to determine the extent of axial conduction on the local Nusselt number. The conductivity ratio ($k_{sf}$) is defined as the ratio of thermal conductivity of the microtube wall ($k_s$) to that of the working fluid ($k_f$). The axial coordinate, z, in non-dimensional form is as follows:

$$Z^* = \frac{Z}{Re \cdot Pr \cdot D_h} \tag{3.10}$$

The non-dimensional local heat flux at the fluid-solid interface is given by:

$$\Phi = \frac{q''}{q''_w} \tag{3.11}$$

where, $q''$ is the local heat flux transferred at the solid-fluid interface along the tube length and $q''_w$ is heat flux on the outer surface of the tube due to constant temperature boundary condition at outer surface along the tube length. The dimensionless bulk fluid and tube inner wall temperatures are given by:

$$\Theta_w = \frac{(T_w - T_{fi})}{(T_{fo} - T_{fi})} \tag{3.12}$$

$$\Theta_f = \frac{(T_f - T_{fi})}{(T_{fo} - T_{fi})} \tag{3.13}$$

Where, $T_{fi}$ and $T_{fo}$ are the average bulk fluid temperature at the tube inlet and outlet respectively; $T_f$ is the average bulk fluid temperature at any location and $T_w$ is the wall temperature at the same Location. The local Nusselt number is then given by:

$$Nu_z = \frac{h_z \cdot D}{k_f} \tag{3.14}$$

where, the local heat transfer coefficient is given by:

$$h_z = \frac{q''_z}{(T_w - T_f)} \tag{3.15}$$

The average Nusselt number over the channel length is given by

$$\overline{Nu} = \int_0^L Nu_z dz \tag{3.16}$$

# Chapter 4

## Results and discussion

As stated in Chapter 3, while the inner radius of the microtube is kept constant, the thickness of the tube wall in the radial direction (refer to Fig. 3.2) is varied to understand the effect of wall thickness on the heat transfer behavior. As the thickness of the solid wall increases, the boundary on which constant wall temperature is applied moves away from the actual fluid-solid interface.

For flow through a channel subjected to either constant wall heat flux or constant wall temperature, maximum heat transfer coefficient will occur if constant heat flux is experienced at the fluid–solid interface of the channel. Under ideal conditions (zero wall thickness) if constant wall heat flux is applied to a circular tube, it will lead to maximum value of Nusselt number for fully developed laminar flow i.e. Nu = 4.36. For similar condition and constant wall temperature boundary condition, the fully developed Nusselt number will be equal to Nu = 3.66. Practically every channel will have some finite wall thickness and because of conjugate heat transfer conditions it is not guaranteed to have the same boundary condition at the solid-fluid interface which is applied on the outer surface of the tube. The objective of this work is to find the actual boundary condition experienced at the solid-fluid interface of a microtube subjected to partial heating by constant wall temperature at its outer surface.

The parameters of interest are axial variation of wall temperature, bulk fluid temperature, and local Nusselt number. First, "Case-1" i.e. heating the microtube over its full length is considered. The axial variation of bulk fluid and wall temperature under ideal condition was presented in Fig. 1.1. Figure 4.1 shows the axial variation of dimensionless wall and bulk fluid temperature as a function of $\delta_{sf}$ and Re. The dotted line represents linear variation of bulk fluid temperature between the inlet and the outlet of the microduct; its limiting values in dimensionless form are 0 and 1. Under ideal conditions, the bulk fluid temperature varies linearly between the inlet and the outlet if the tube is subjected to constant heat flux boundary condition. At lower flow Re (=100) and lower value of $\delta_{sf}$ (=1), the axial variation of bulk fluid temperature can be seen to be away from linear variation (see Fig. 4.1), and close to the parabolic variation (see Fig. 1.1(b)) which is the case when the tube is subjected to constant wall temperature condition. The results in Fig. 4.1 are independent of $k_{sf}$ except at very low value of $k_{sf}$ = 2.26. Secondly, the wall temperature is almost constant throughout the length of the tube except near the inlet; due to developing flow. A comparison of Fig. 4.1(a) and Fig. 1.1(b) leads to the conclusion that the solid-fluid interface for this case experiencing constant wall temperature; which is exactly equal to the actual boundary condition applied on the outer surface of the tube. This means for this case there is no axial flow of heat to distort the boundary condition at the solid-fluid interface.

Next, the value of $\delta_{sf}$ increased from 1 to 10, while all other parameters remaining the same as in Fig. 4.1(a). Now, it can be observed in Fig. 4.1(b) that the results are no more independent of $k_{sf}$. Secondly, the bulk fluid temperatures are comparatively closer to the dotted line, indicating that the actual boundary condition at the solid-fluid interface is drifting away from isothermalization. This can also be confirmed from the values of wall temperatures; which are no more constant for lower values of $k_{sf}$. This indicates higher wall thickness and lower conductive

wall material drifts from actual boundary condition first.

Figure 4.1(c) and 4.1(e) represent corresponding diagram of Fig. 4.1(a) at higher flow Re. Similarly, Figure 4.1(d) and 4.1(f) represent corresponding diagram of Fig. 4.1(b) at higher flow Re. It can be seen that the higher the flow Re, the more the bulk fluid temperatures are close to

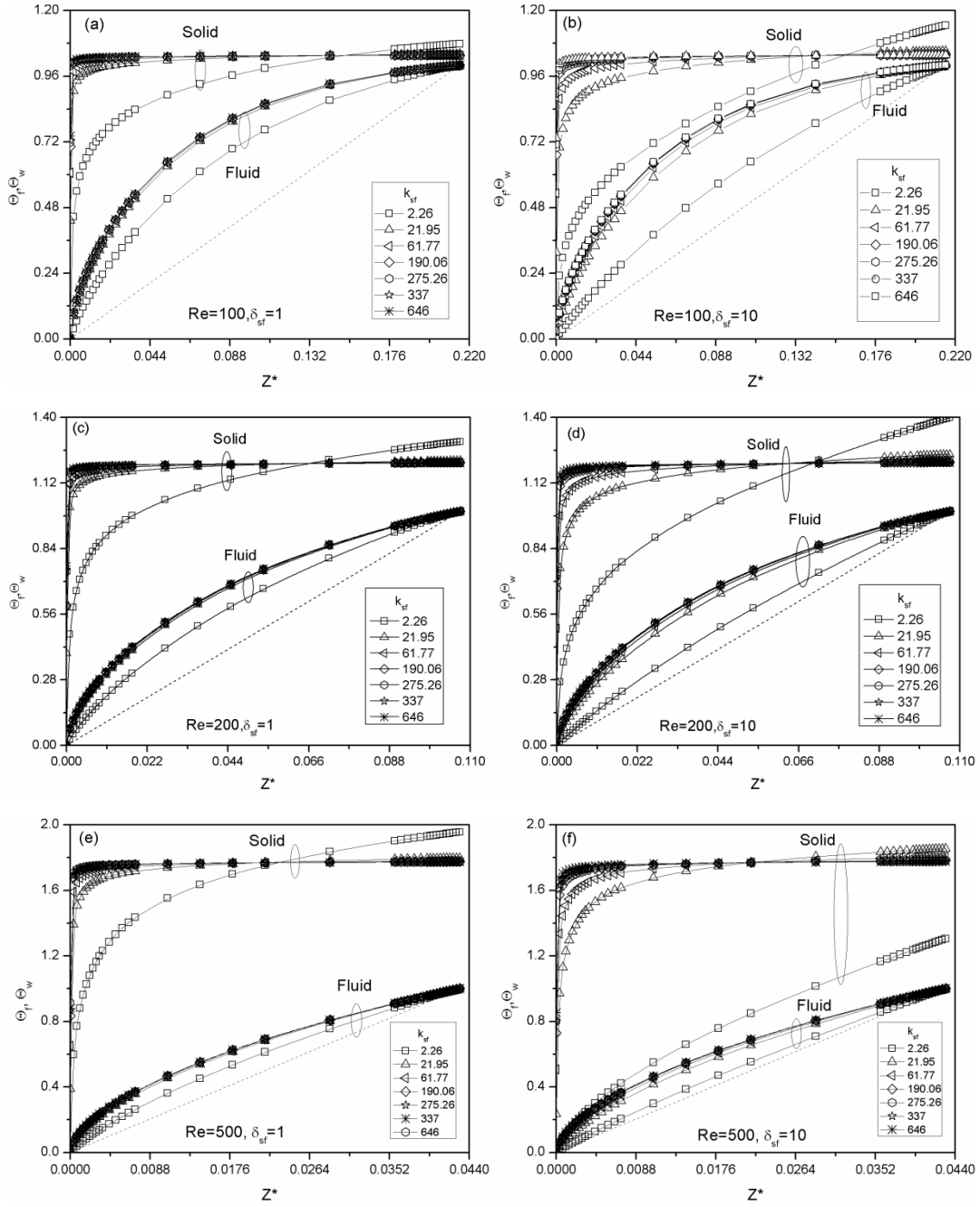


Fig. 4.1: Axial variation of dimensionless wall temperature and bulk fluid temperature as a

function of $\delta_{sf}$, $k_{sf}$ and Re (for heating as per Case-1).

the dotted line. Next, it can be observed that with further increasing wall thickness i.e. $\delta_{sf}$, the gap between the wall and the fluid temperature becomes constant in the fully developed region especially for lower value of $k_{sf}$.

Fig. 4.2 shows the corresponding plot of Fig. 4.1, for Case-2 (refer Fig. 3.2(b)) where the dimensionless wall temperature and bulk fluid temperature are varying along the length of the microtube. In Case-2, 6 mm length is insulated from the inlet and the outlet end of the microtube. Ideally wall temperature in the first 6mm and the last 6 mm length should be equal to fluid inlet temperature and bulk fluid temperature in the first 6mm should be equal to fluid inlet temperature. The two vertical dotted lines represent the heating length of the microtube. Because of finite conductivity of the wall material, there will be conduction of heat in the wall near the inlet in a direction opposite to the direction of flow of fluid. This can be observed in Fig. 4.2(a) where the bulk fluid temperature starts rising above zero in between z = 0 to 6 mm (i.e. $z^* = 0$ to 0.0215). For lowest $k_{sf}$ (= 2.26) the value of bulk fluid temperature as well as the wall temperature are almost equal to zero and constant in the range z = 0 to 6 mm (i.e. $z^* = 0$ to 0.0215). With increasing $k_{sf}$, the value of both the wall and the bulk temperature starts rising in the insulated region near the inlet. This is due to axial back conduction in the wall of the microtube. Higher the value of $k_{sf}$, lower the resistance to flow of heat by conduction; thus more the rise in both the wall and the bulk fluid temperature.

Figure 4.2(a) corresponds to $\delta_{sf} = 1$ while Fig. 4.2(b) corresponds to $\delta_{sf} = 10$. Higher area of cross-section of solid leads to lower thermal resistance to axial conduction under same conditions. This can be observed by direct comparison between Fig. 4.2(a) and 4.2(b). In Fig. 4.2(b) the slope of wall temperature in the region z < 6 mm (or $z^* < 0.0215$) is higher compared

to its counterpart in Fig. 4.2(a). Next, for higher flow Re, the bulk fluid temperature drifts from parabolic towards linear variation in between the two dotted vertical lines, which corresponds to the heated zone. This indicates higher flow Re leads to the condition at the solid-fluid interface more towards constant wall heat flux than constant wall temperature.

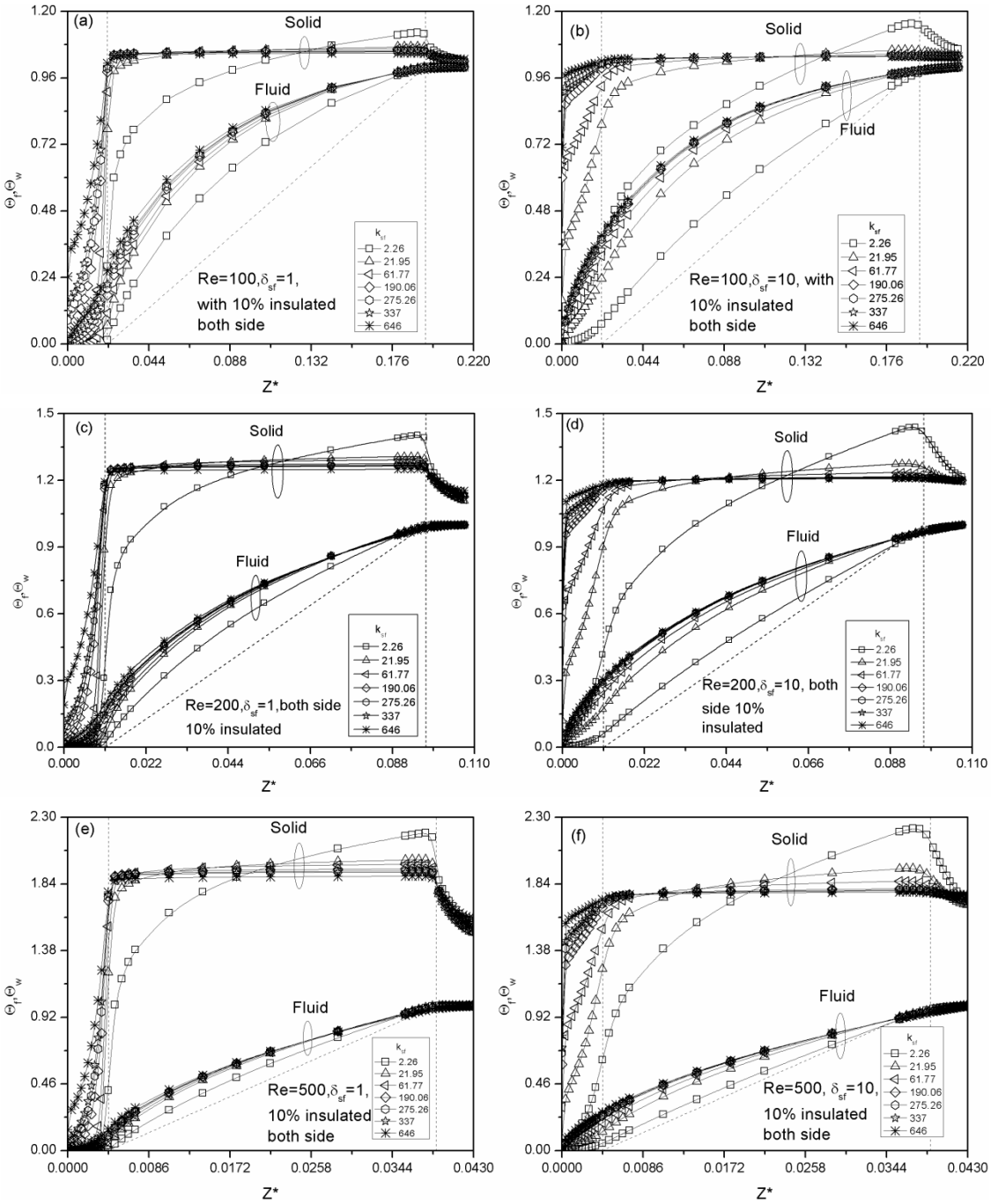


Fig. 4.2: Axial variation of dimensionless wall temperature and bulk fluid temperature as a

function of $\delta_{sf}$, $k_{sf}$ and Re (for heating as per Case-2).

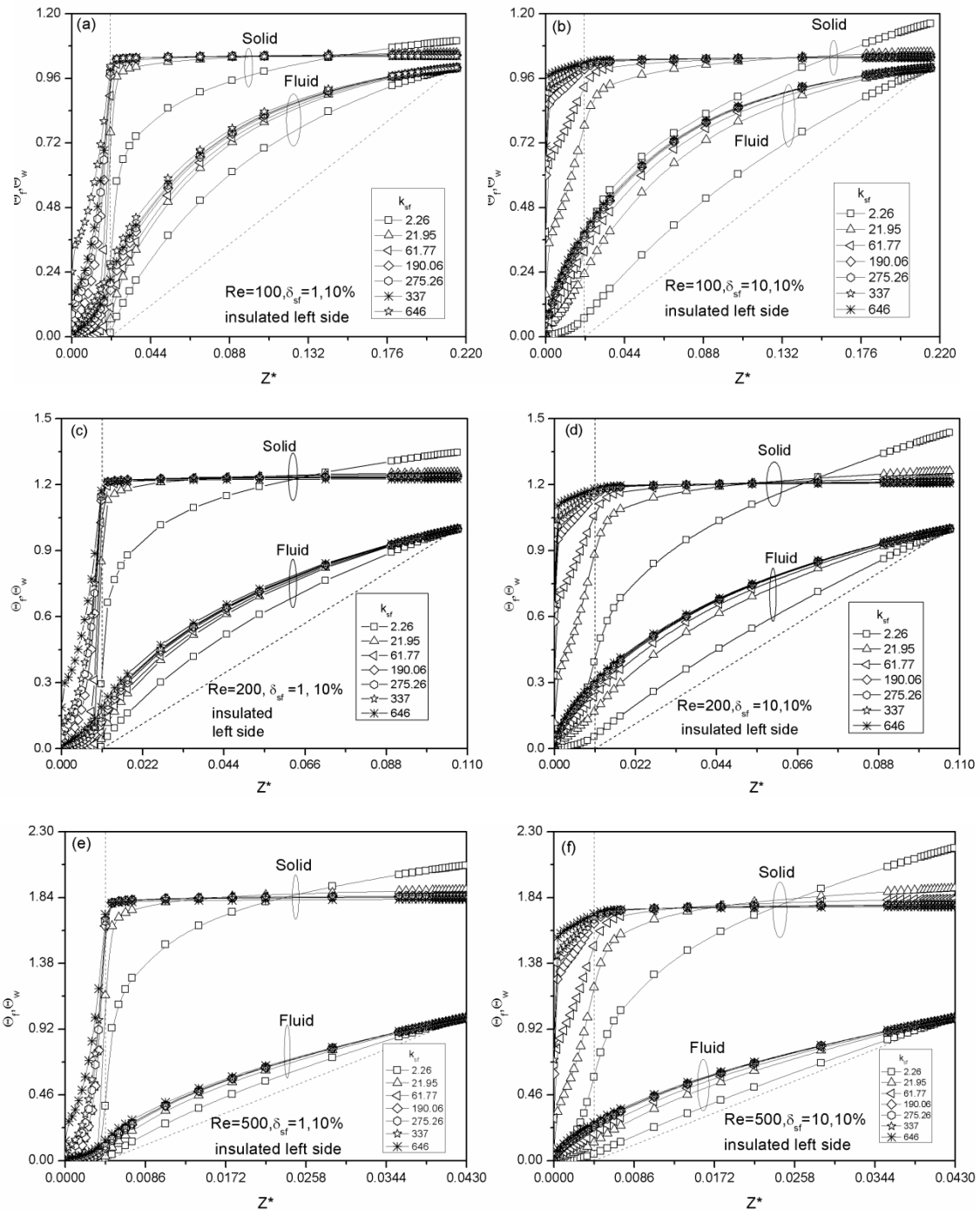


Fig. 4.3: Axial variation of dimensionless wall temperature and bulk fluid temperature as a function of $\delta_{sf}$, $k_{sf}$ and Re (for heating as per Case-3).

The microtube is insulated on its outer surface in the region z > 54 mm (i.e. $z^* > 0.194$). In

this region the bulk fluid temperature remains almost constant for the case of $\delta_{sf}$ = 1 (see Fig. 4.2(a)). This is because there is no heat addition in this region. Secondly, the wall temperature is slightly higher than the bulk fluid temperature, thus there will be almost no heat transfer from wall to the fluid except at the lowest $k_{sf}$. For $k_{sf}$ = 2.26, the difference between wall and fluid temperature is maximum compared to other $k_{sf}$ values at the start of end insulation. Therefore for $k_{sf}$ = 2.26, the wall temperature starts to decrease in the end insulated region in the direction of flow of fluid. For higher flow Re, the difference between the bulk fluid and the wall temperature is higher at z = 54 mm (i.e. $z^*$ = 0.194) compared to lower flow Re (compare between Fig. 4.2(e) and Fig. 4.2(a)). Therefore in this case the wall temperature starts decreasing in the direction of flow of fluid due to transfer of heat from the wall to the fluid.

Fig. 4.3 presents axial variation of dimensionless wall and bulk fluid temperature for Case-3 heating in which 6 mm is insulated from the inlet (as shown in Fig. 3.2(c)) and the remaining part is subjected to constant wall temperature. Geometrically this case is similar to Case-2 heating minus the insulation length of 6mm provided near the outlet. Therefore the axial variation of both wall and bulk fluid temperature in Fig. 4.3 are almost same as the part of the curve to the left of the right side vertical dotted line in Fig. 4.2.

Fig. 4.4 presents axial variation of dimensionless wall and bulk fluid temperature for Case-4 heating in which 6 mm is insulated from the outlet (as shown in Fig. 3.2(d)) and the remaining part is subjected to constant wall temperature. Geometrically only the heating portion of Case-4 is similar to Case-1 heating. Therefore the axial variation of both wall and bulk fluid temperature in Fig. 4.4 which are to the left of the vertical dotted line are almost same as the curves presented in Fig. 4.1.

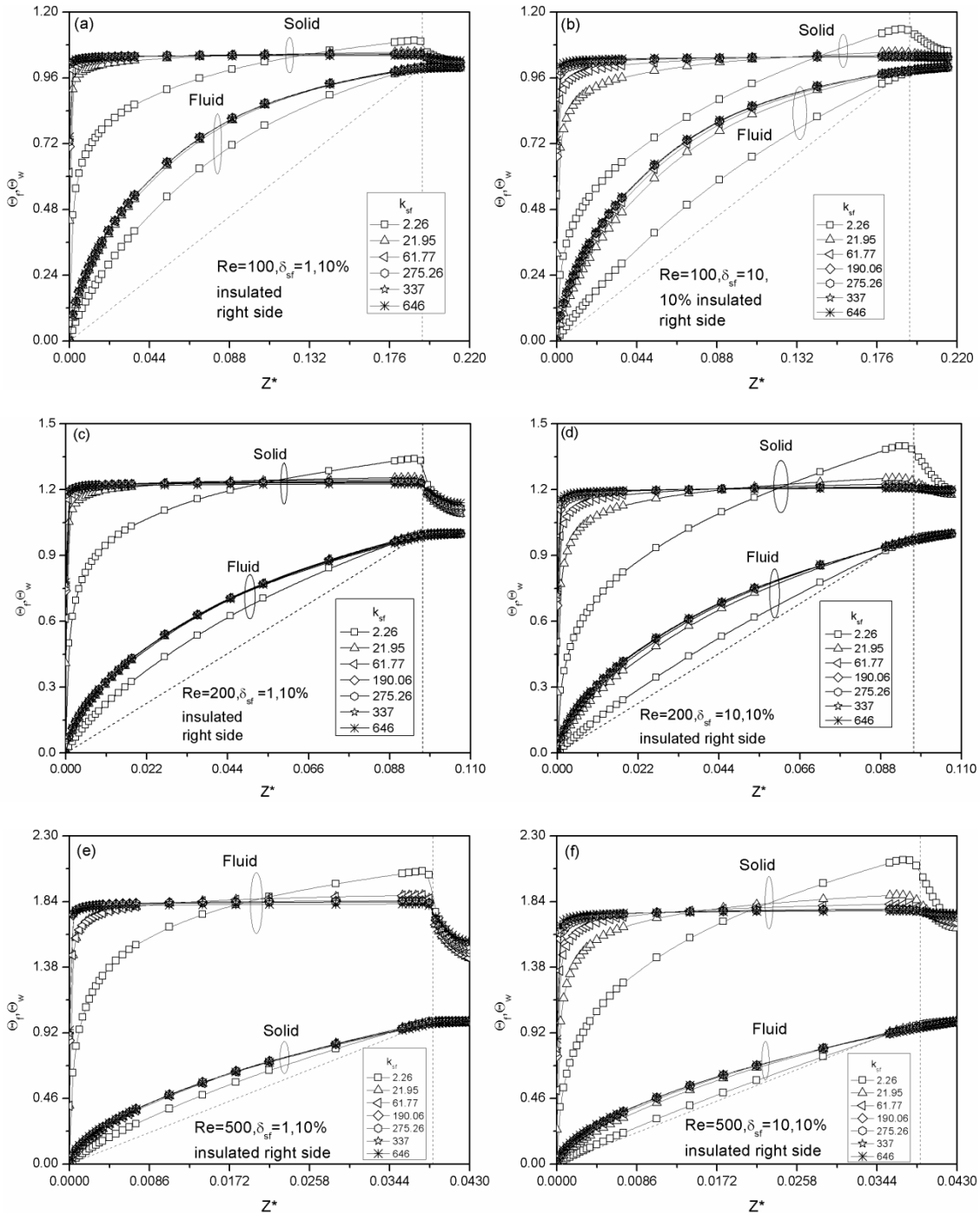


Fig. 4.4: Axial variation of dimensionless wall temperature and bulk fluid temperature as a function of $\delta_{sf}$, $k_{sf}$ and Re (for heating as per Case-4).

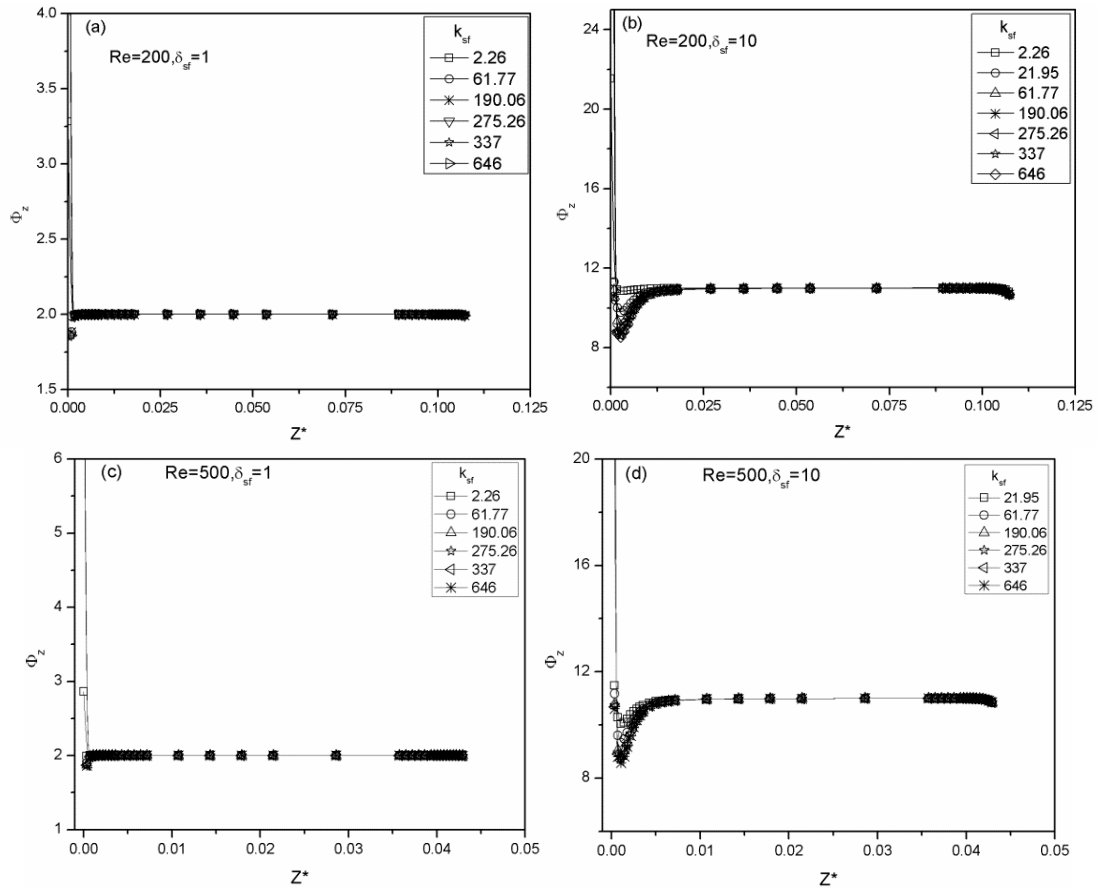


Fig. 4.5: Axial variation of dimensionless heat flux as a function of $\delta_{sf}$, $k_{sf}$ and Re (for heating as per Case-1).

From all the cases considered in this study, it is clearly evident that the actual heat flux experienced at the fluid-solid interface is approximately axially uniform/constant irrespective of the conductivity ratio ($k_{sf}$), thickness ratio ($\delta_{sf}$). At higher thickness ratio ($\delta_{sf}$), the actual heat flux experienced at the fluid-solid interface is much more than for lower thickness ratio ($\delta_{sf}$). This qualitative pattern of axial variation in heat flux is due to the fact that low thermal conductivity ratio and lower thickness ratio ($\delta_{sf}$) leads to higher axial thermal resistance in the wall and vice versa. Accordingly, at higher $\delta_{sf}$ low axial thermal resistance of the wall leads to significant back conduction; this effect becomes naturally more prominent with increase in conductivity ratio

($k_{sf}$). As we can see in Fig. 4.5(a) and Fig. 4.5(b) we can see that for some distance from inlet in the direction of axial location the value of ratio of heat flux is approximately constant for all $k_{sf}$ with value nearly equal to 2 and 10 for the case of $\delta_{sf}$ = 1 and 10 respectively. As well as this result is also same for higher Reynold number as shown in Fig. 4.5(c) and Fig. 4.5(d). So from these plots we can say that value of heat flux at solid-fluid interface is mainly depend on wall thickness when at outer periphery constant wall temperature is applied.

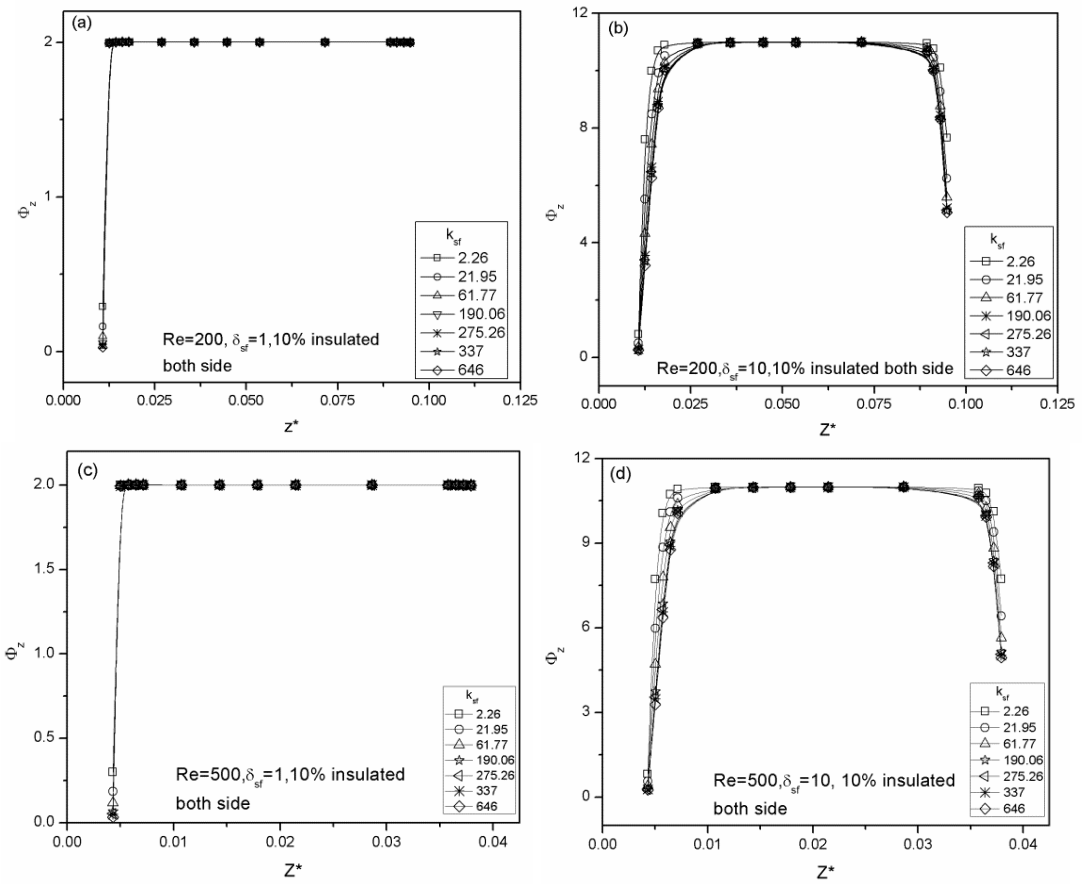


Fig. 4.6: Axial variation of dimensionless heat flux as a function of $\delta_{sf}$, $k_{sf}$ and Re (for heating as per Case-2).

Analogous observations were reported by Zhang et al. (2010), who applied a constant temperature boundary condition at the outer surface of a circular tube (case1 refer to Fig. 3.2(a))and found that the dimensionless heat flux at the fluid-solid boundary tends to become

constant when axial conduction in the tube wall dominates.

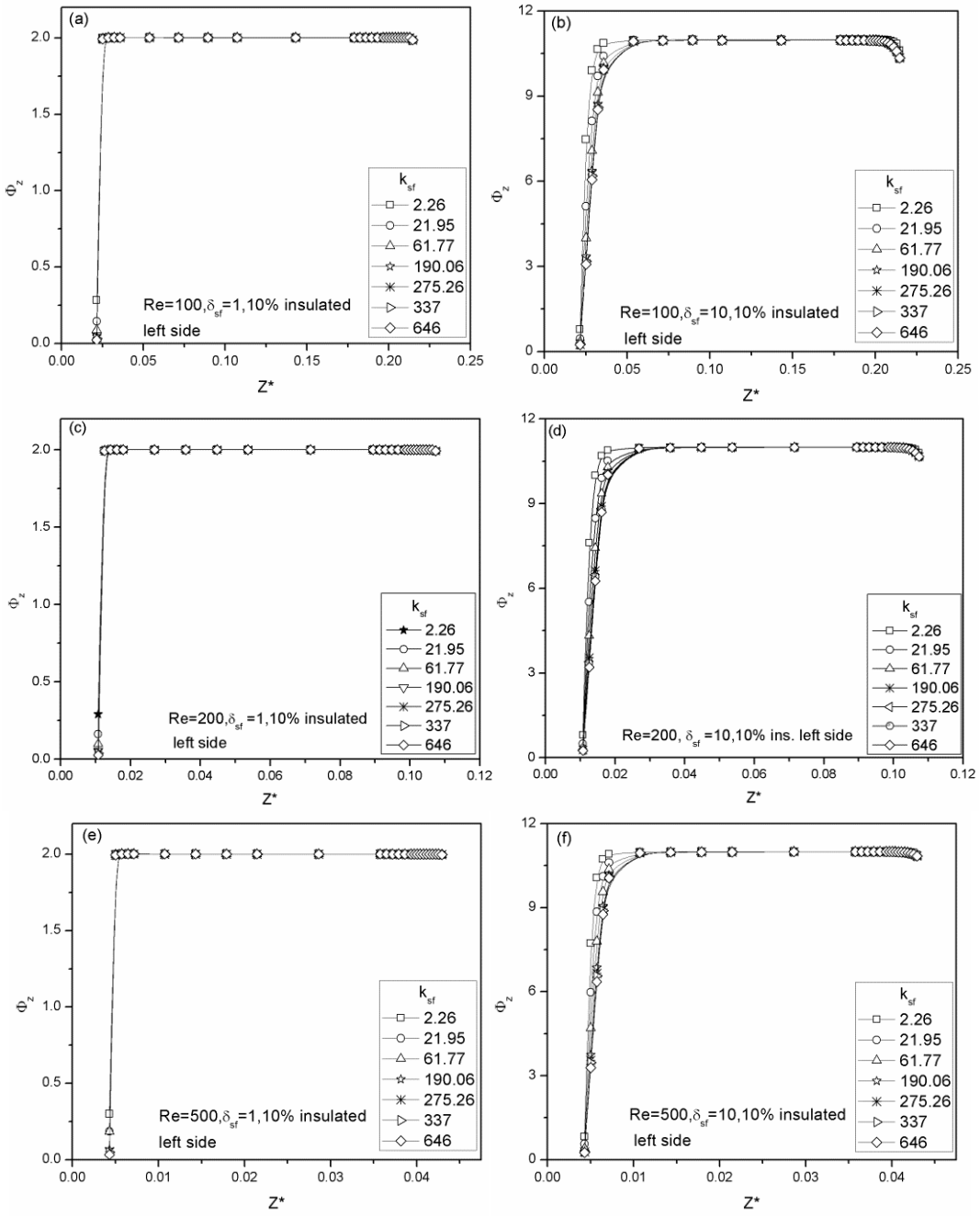


Fig. 4.7: Axial variation of dimensionless heat flux as a function of $\delta_{sf}$, $k_{sf}$ and Re (for heating as per Case-3).

From fig. 4.5 - 4.6 it is clear that for all condition as illustrated earlier as four cases and shown in Fig. 3.2, the heat flux( $\Phi$ ) is strong function of $\delta_{sf}$ . But it is a week function of Re and $k_{sf}$ due

to axial back condition.

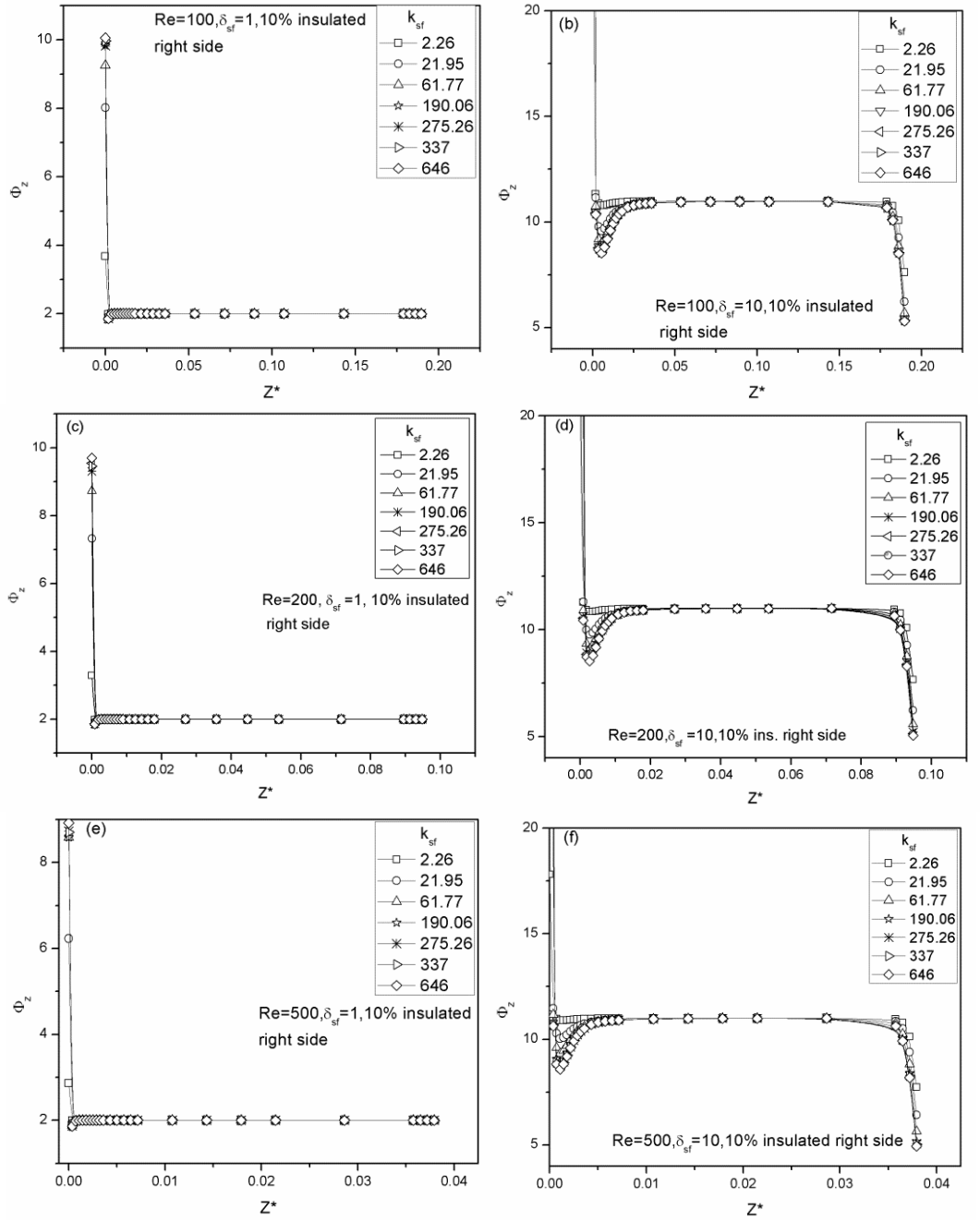


Fig. 4.8: Axial variation of dimensionless heat flux as a function of $\delta_{sf}$, $k_{sf}$ and Re (for heating as per Case-4).

The direct implication of the axial variation of dimensionless wall and bulk fluid temperature, (as in Fig. 4.1 to Fig. 4.4) and dimensionless wall heat flux (as in Fig. 4.5 to Fig. 4.8) decides the

value of local Nusselt number, which are presented next in Fig. 4.9 to Fig. 4.12.

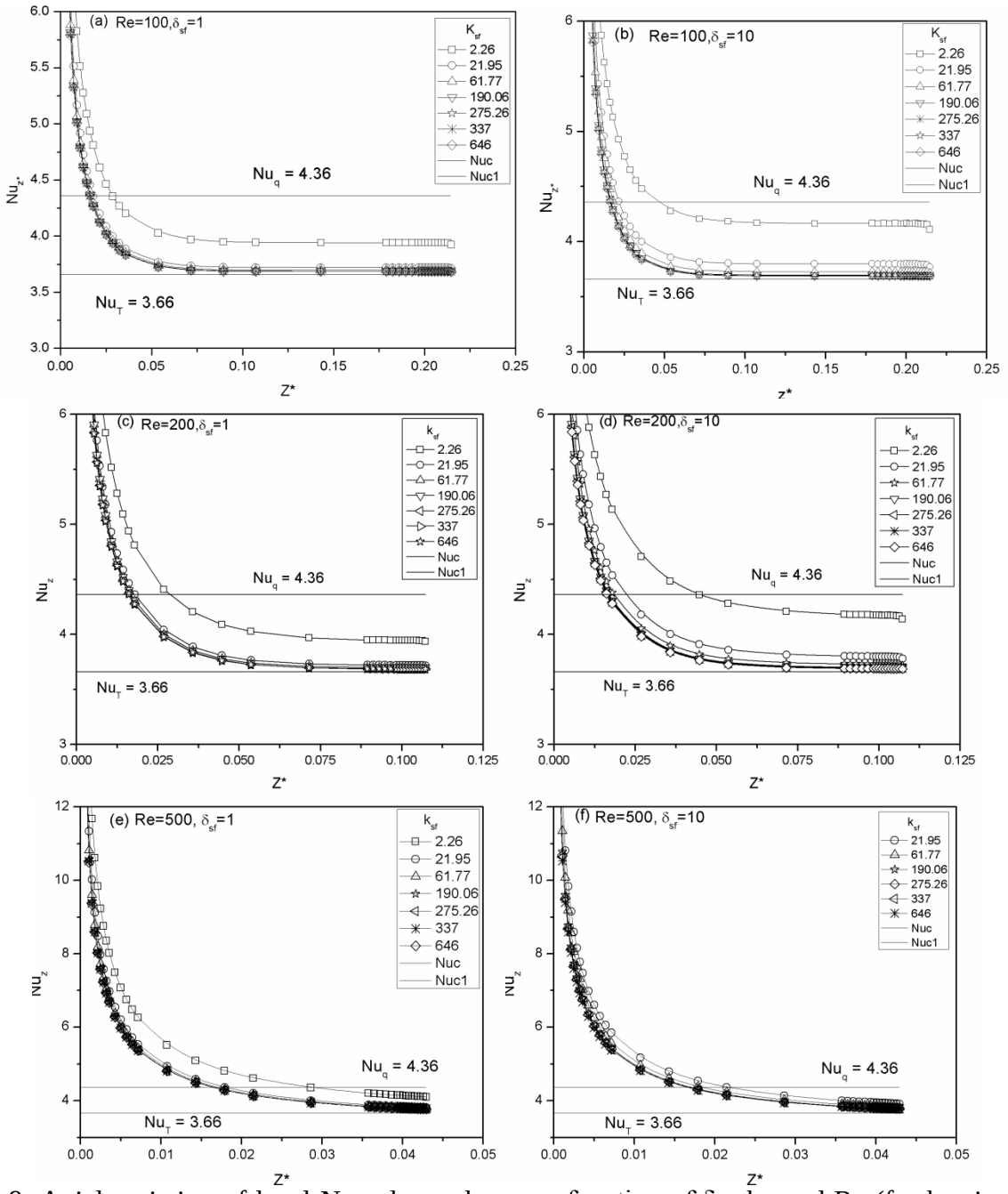


Fig. 4.9: Axial variation of local Nusselt number as a function of $\delta_{sf}$, $k_{sf}$ and Re (for heating as per Case-1).

Figure 4.9 represents axial variation of local Nusselt number for the microtube subjected to Case-1 heating, which are corresponding diagrams of Fig 4.1 and Fig. 4.5. As discussed earlier,

if the boundary condition experienced at the solid-fluid interface is close to constant wall heat flux, then the local Nusselt number in the fully developed zone will converge close to $Nu_q$ = 4.36. And if the boundary condition experienced at the solid-fluid interface is close to constant wall temperature, then the local Nusselt number in the fully developed zone will converge close to $Nu_T$ = 3.66. These two limiting values of Nu are represented in Fig. 4.9 by two horizontal solid lines.

For low flow Re and lower wall thickness, the fully developed Nusselt numbers ($Nu_{fd}$) are slightly higher than $Nu_T$ and the value of $Nu_{fd}$) increases with decreasing value of $k_{sf}$, which can be observed in Fig 4.9(a). Secondly, as the wall thickness increased from $\delta_{sf}$ = 1 to 10, keeping all other parameters unchanged, the local Nu value increases at any axial location and for any value of $k_{sf}$. But this increase is sensitive to $k_{sf}$, and the lower the $k_{sf}$, the higher the increase in local Nu. This can be observed in Fig. 4.9(b).

For second case shown in Fig. 3.2(b) the plot of local Nusselt number is shown in Fig. 4.10. It is clear from here that the behavior of local Nusselt number plot in the direction of axial location is different at the insulated position at both side i.e. at inlet and outlet. Here at inlet the value of local Nusselt number is constant up to length of insulation and then it decreases up to the value for fully developed flow and again it decreases suddenly at the outlet and again increases in the insulated region.

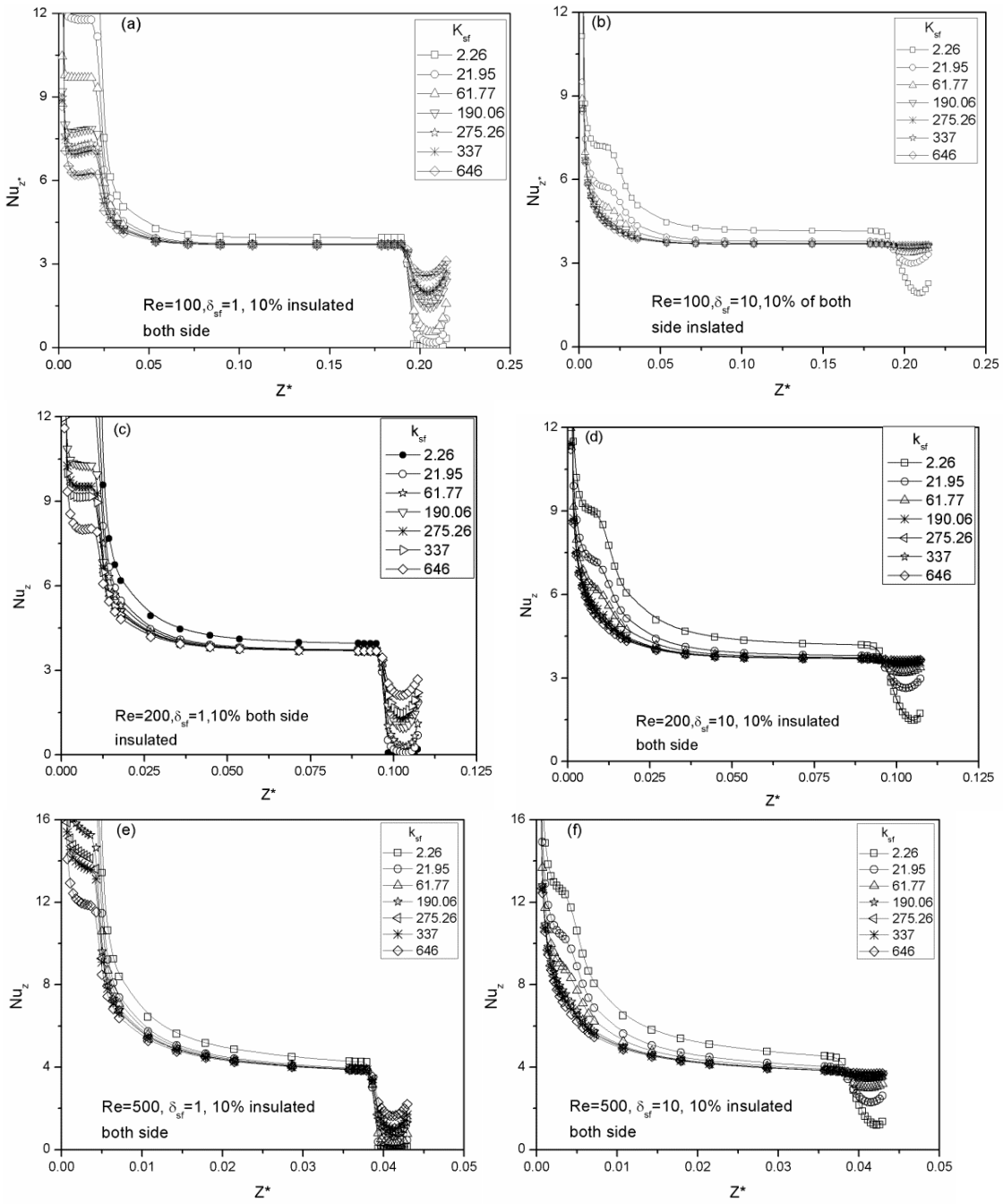


Fig. 4.10: Axial variation of local Nusselt number as a function of $\delta_{sf}$, $k_{sf}$ and Re (for heating as per Case-2).

It can be observed that for higher $k_{sf}$ and $\delta_{sf}$ (in Fig. 4.10(e)) the boundary condition at the fluid-solid interface increasingly approach the trend closer to an constant heat flux boundary

condition, although isothermal boundary condition is applied at the outer part of microtube. The axial variations of local Nusselt number are presented in Fig. 4.9-4.12 for a wide variation in thermal conductivity ratio ($k_{sf}$), Flow(Re) and the thickness ratio ($\delta_{sf}$).

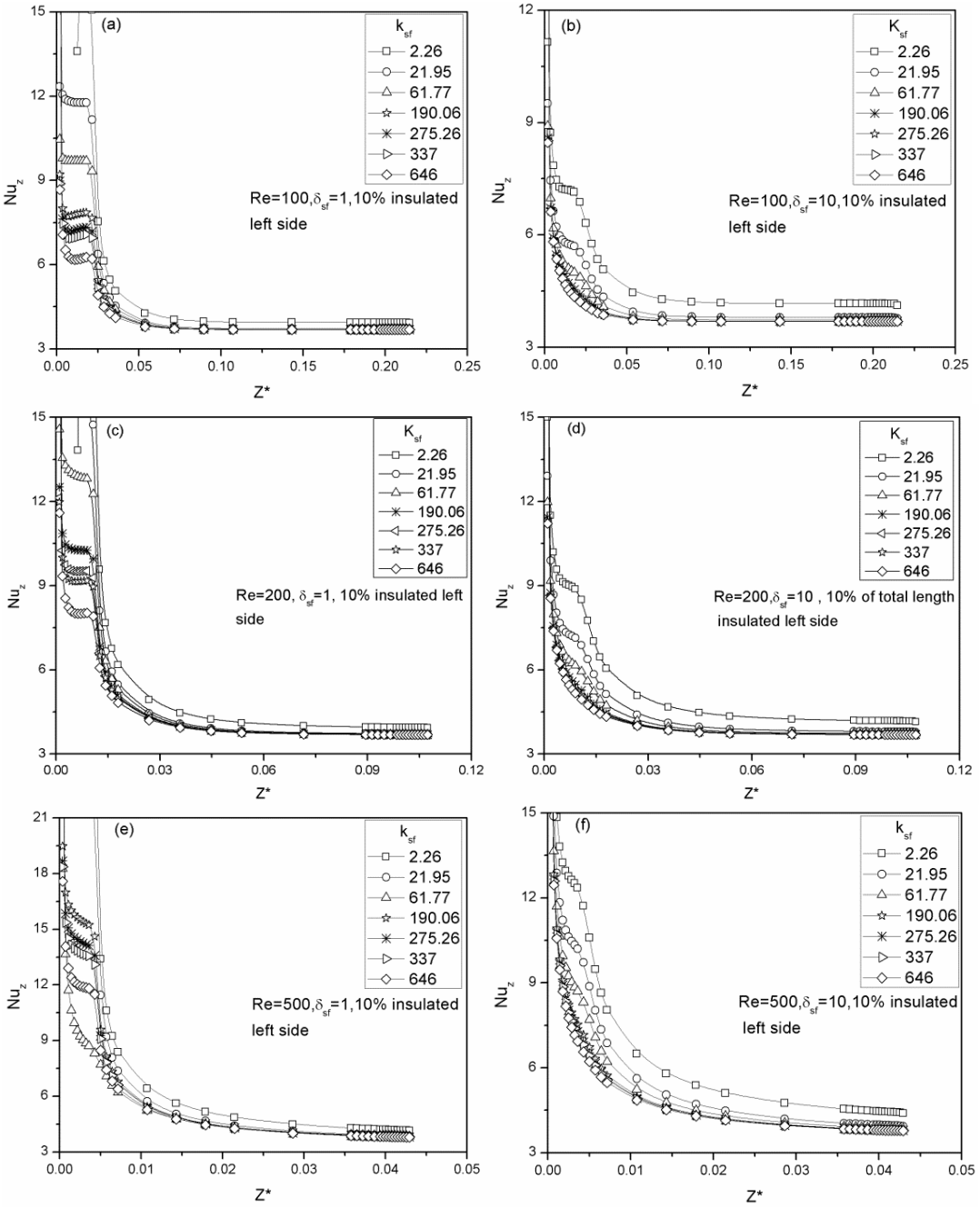


Fig. 4.11: Axial variation of local Nusselt number as a function of $\delta_{sf}$, $k_{sf}$ and Re (for heating as per Case-3).

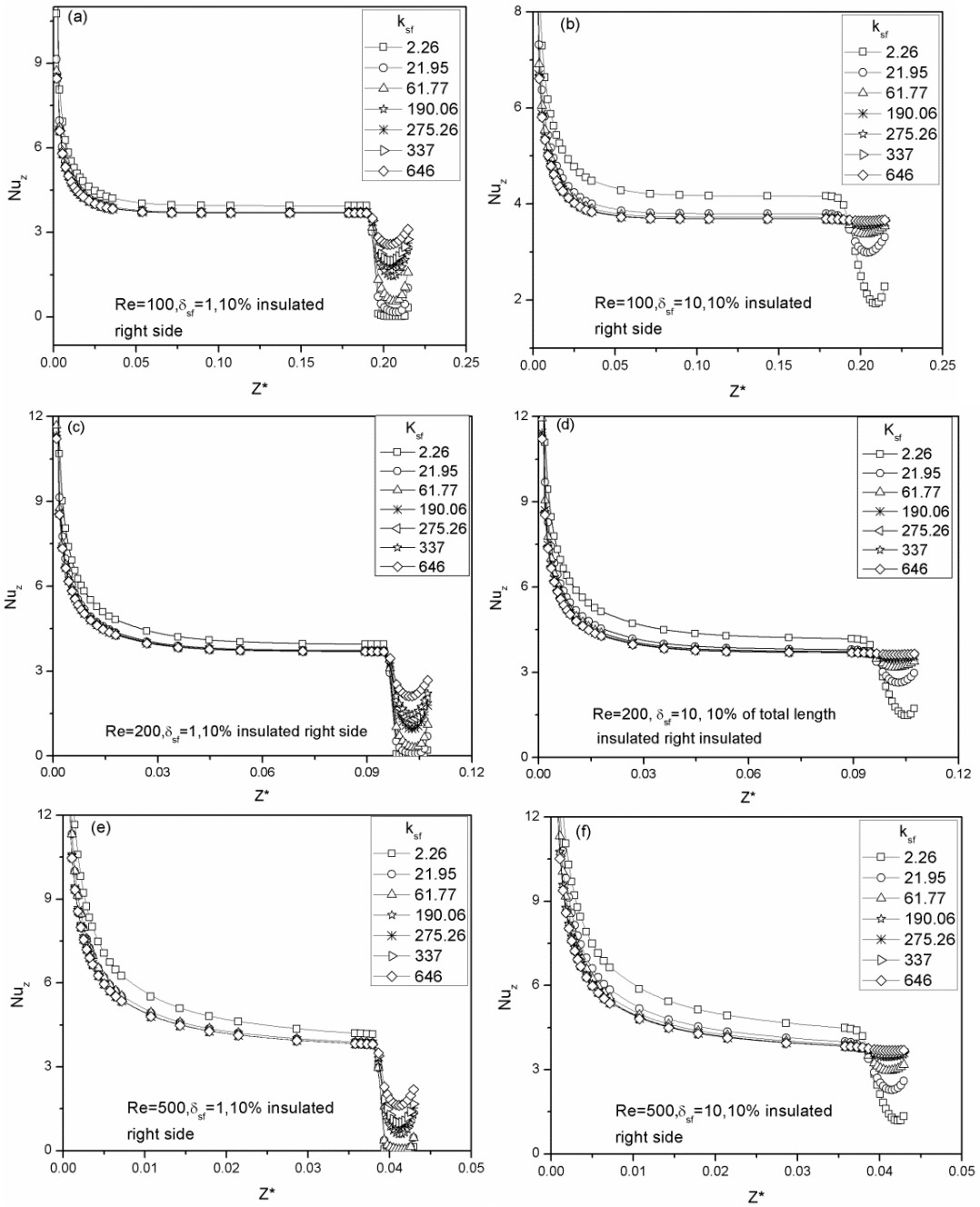


Fig. 4.12: Axial variation of local Nusselt number as a function of $\delta_{sf}$, $k_{sf}$ and Re (for heating as per Case-4).

As it is already discussed earlier that case 3 is showing similar nature like case 2 up the heating region towards outlet which can also be seen in Fig.4.11 and Fig.4.10 respetively.

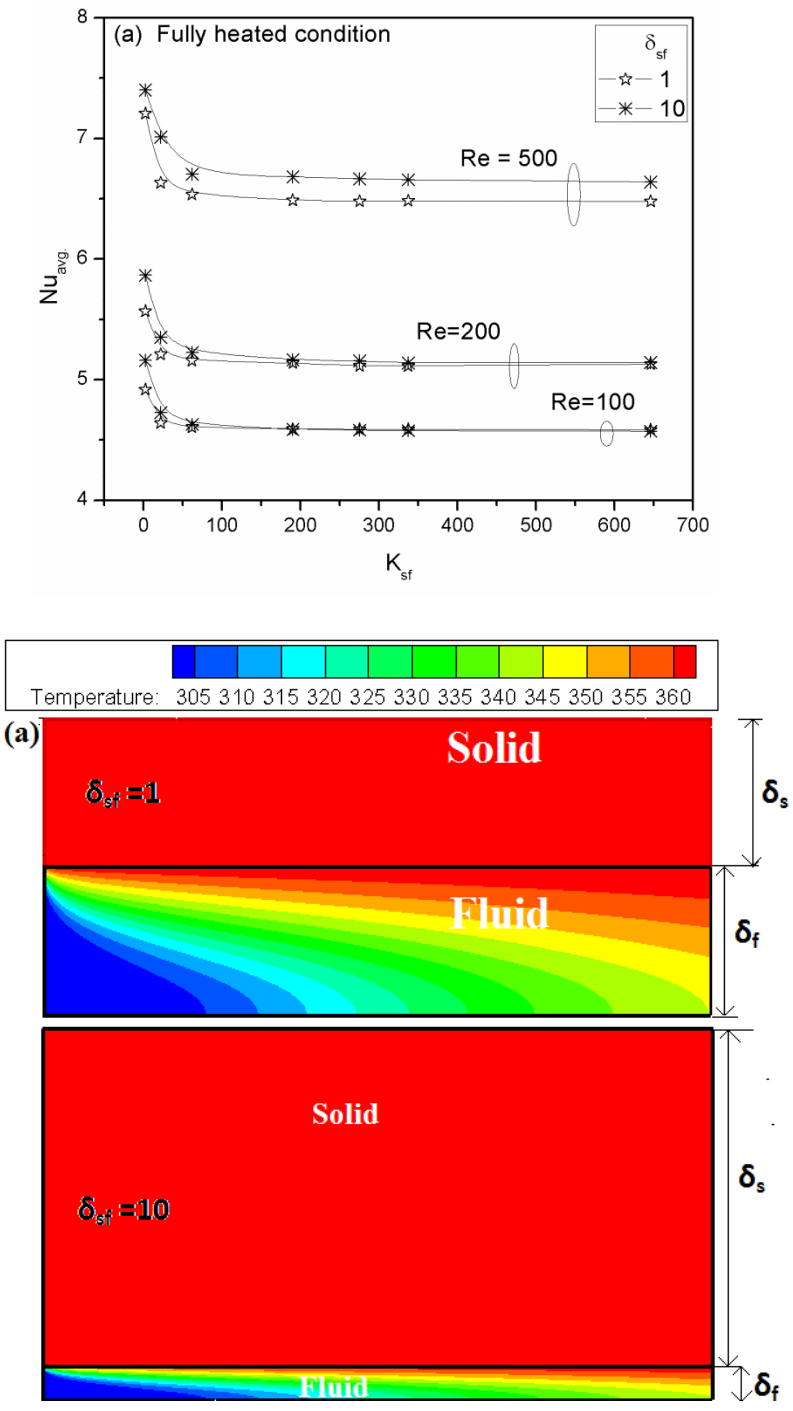


Fig.(4.13). (a) Variation of average Nusselt number with $k_{sf}$ ,for (Re = 100-500),&( $\delta_{sf}$ = 1-10) and temperature contours for fully heated condition.

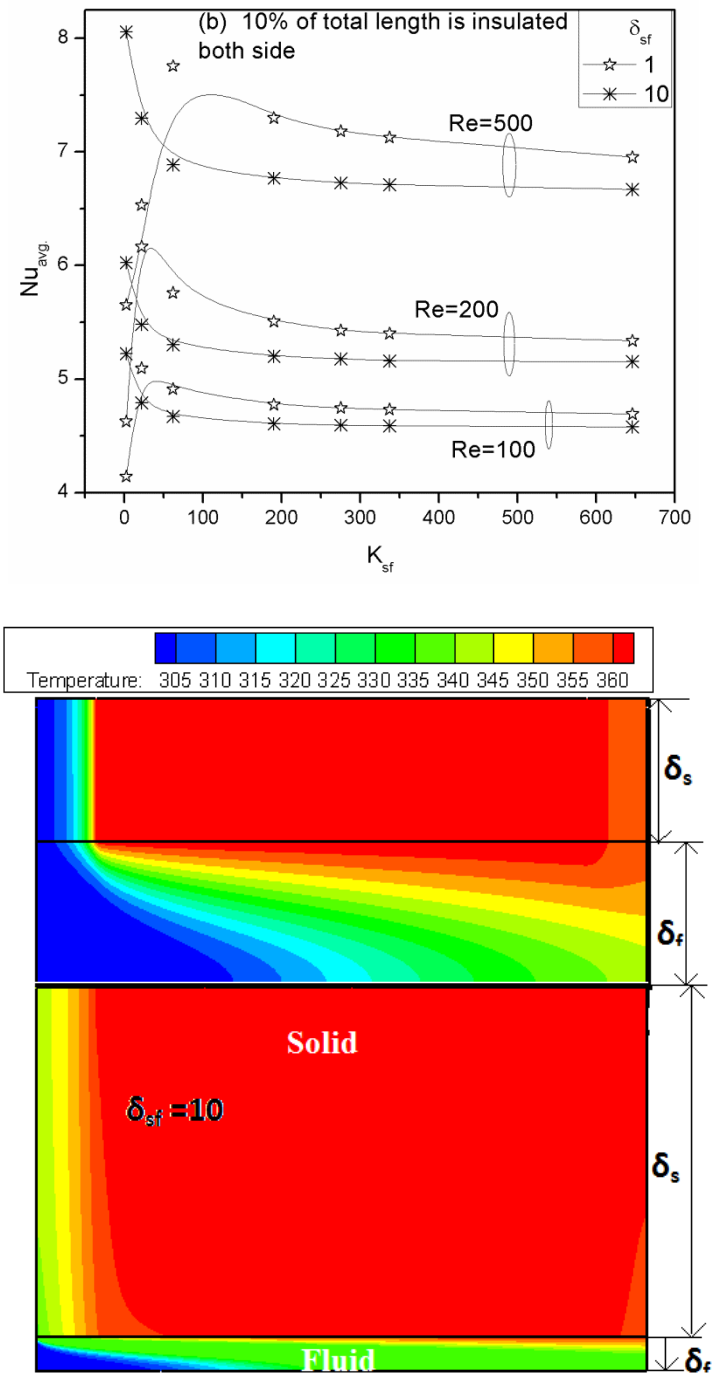


Fig.(4.13). (b) Variation of average Nusselt number with $k_{sf}$, for (Re = 100-500),&( $\delta_{sf}$ = 1-10) and temperature contours for 10% of total length is insulated both side boundary condition.

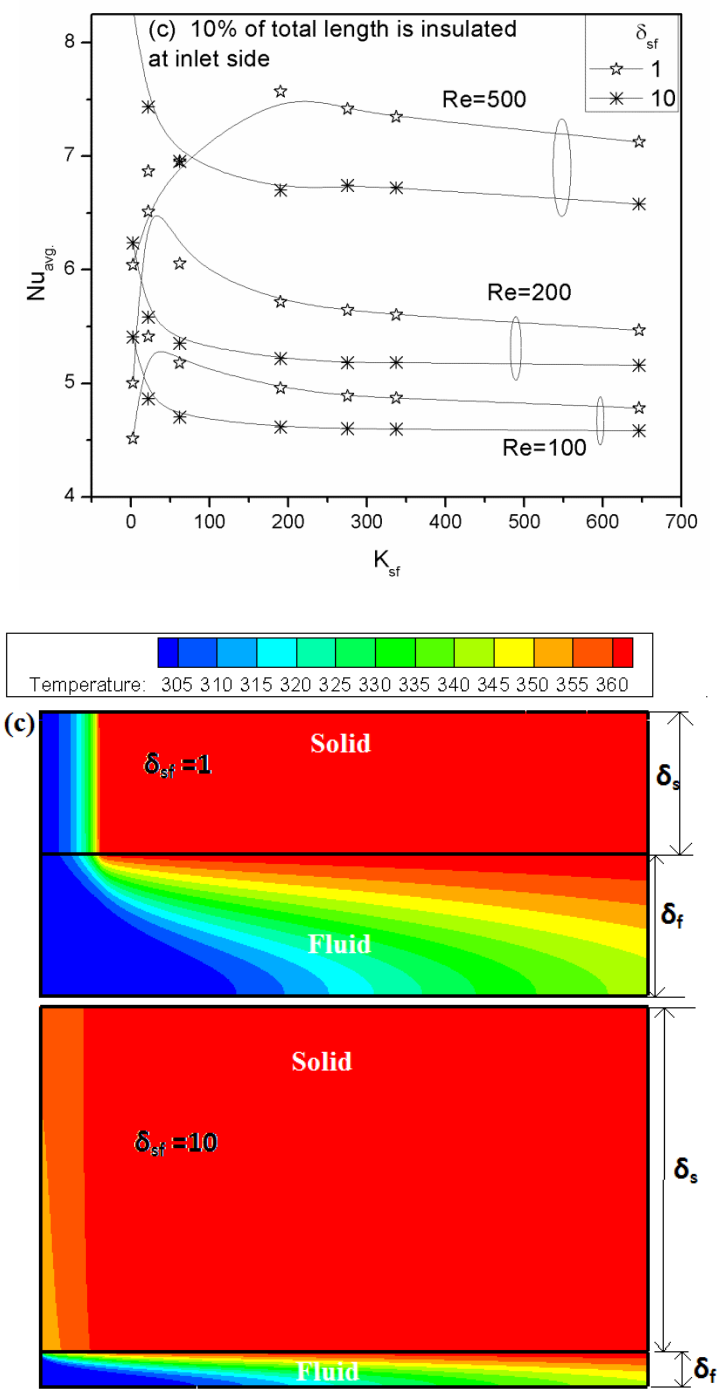


Fig. (4.13). (c) Variation of average Nusselt number with $k_{sf,}$ for (Re = 100-500), &( $\delta_{sf}$ = 1-10) and temperature contours for 10% of total length is insulated at inlet.

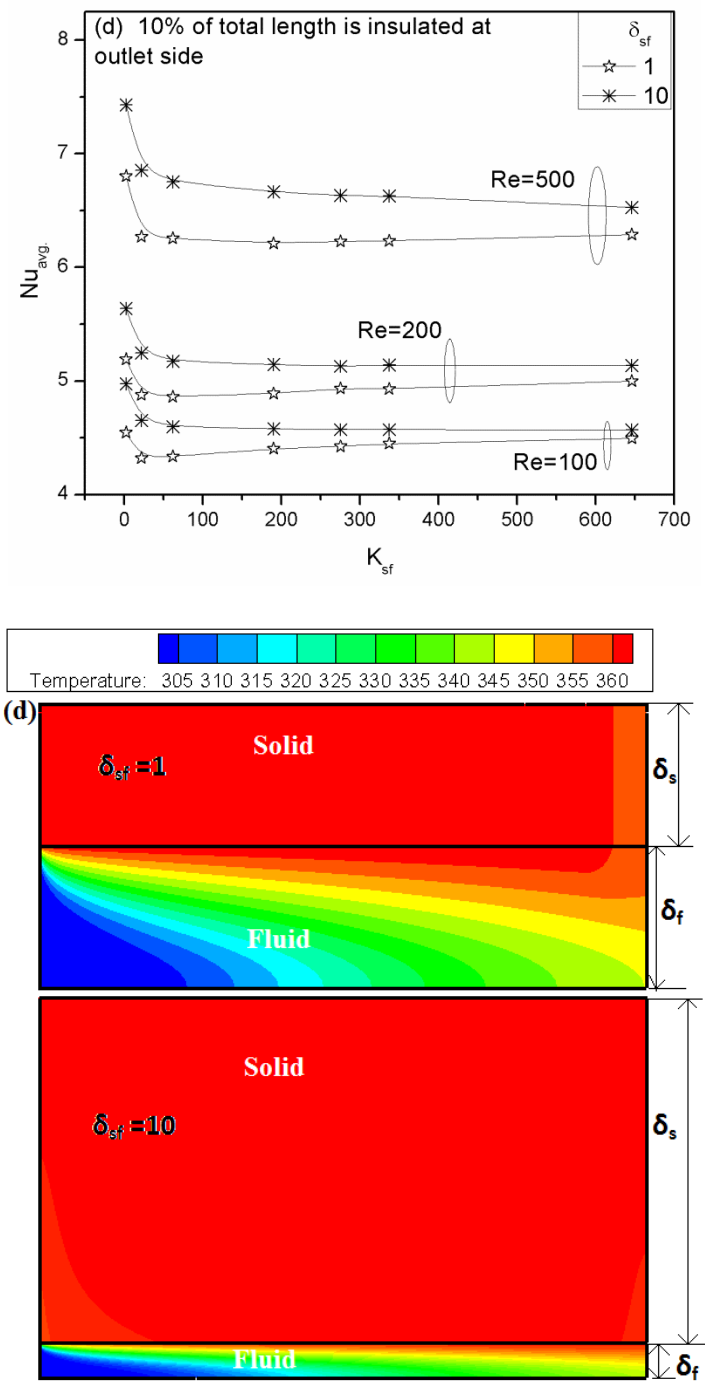


Fig. (4.13). (d) Variation of average Nusselt number with $k_{sf,}$ for (Re = 100-500), & ( $\delta_{sf}$ = 1-10) and temperature contours for 10% of total length is insulated at outlet.

In the thicker wall the axial variation of wall temperature at the solid-fluid interface drifts

more towards the trend of constant heat flux rather than constant wall temperature. This causes higher Nusselt number compared to thinner tube wall thickness. It is very clear from fig.4.13 that the value of average Nusselt number is maximum at very low $k_{sf}$ in the case of full heating and in another case when the outer periphery of the pipe is insulated at outlet side (shown in fig.3.2a and 3.2d respectively). where as in the case when the outer periphery of the pipe is insulated at both outlet side and inlet side and another case when only at inlet side is insulated (as shown in fig. 3.2b and 3.2c respectively) the value of average Nusselt number is maximum at an optimum value of $k_{sf}$. So we can say that for case 2 and case 4 for an optimum value of Nusselt number heat transfer will not vary with thickness ratio($\delta_{sf}$).

# Chapter 5

## Conclusion

A numerical analysis has been carried out for internal convective flows in a microtube subjected to conjugate heat transfer situation. This analysis has been carried out to understand the effect of axial wall conduction for simultaneously developing laminar flow and heat transfer in a circular microtube subjected to constant wall temperature boundary condition imposed on its outer surface. Practically in many a situations the two ends or one of the ends of the microtube are insulated because of demand of physical situation. In this background, we have considered for four most practical cases of partial heating of microtubes: (i) the outer surface of the microtube is subjected to constant wall temperature over its full length (ii) 10% of total length at both the inlet and the outlet end are insulated while the remaining length is subjected to constant wall temperature boundary condition (iii) 10% of total length at inlet is insulated while the remaining length is subjected to constant wall temperature boundary condition (iv) 10% of total length at outlet is insulated while the remaining length is subjected to constant wall temperature boundary condition. Simulations have been carried out for a wide range of pipe wall to fluid conductivity ratio ($k_{sf}$: 2 - 646), pipe wall thickness to inner radius ratio ($\delta_{sf}$: 1, 10), and flow Re (100 - 500). The main outcomes of this study are

- For fully heated microtube, it is found that the value of $Nu_{avg}$ is increasing with decreasing value of $k_{sf}$ and the rate of increase of $Nu_{avg}$ is higher for smaller values of $k_{sf}$ ($k_{sf} < 50$). Secondly, while other parameters remaining same, for lower $\delta_{sf}$, $Nu_{avg}$ is higher compared to higher $\delta_{sf}$. The difference between the $Nu_{avg}$ values (corresponding to $\delta_{sf} = 1, 10$) at lower $k_{sf}$ is higher compared to at higher $k_{sf}$ values. Finally, the value of $Nu_{avg}$ increases with increasing flow Re while other parameters are constant.
- The trend observed for the case of partial heating where 6 mm (i.e. 10% of total length) is insulated from the outlet end is qualitatively similar to that observed in case of full heating but with some deviations as outlined below. The value of $Nu_{avg}$ starts decreasing with decreasing value of $k_{sf}$ up to approximately $k_{sf}$ equal to 40. On further decreasing value of $K_{sf}$, value of $Nu_{avg}$ starts increasing rapidly. Thus, there exists an optimum $k_{sf}$ at which $Nu_{avg}$ is minimum for this case. Secondly, the difference between $Nu_{avg}$ values at any $k_{sf}$ is higher compared to the case of full heating.
- For Case-2 heating (i.e. 10 % of total length is insulated near the inlet and the outlet each) the average Nusselt number ($Nu_{avg}$) for higher wall thickness (i.e. $\delta_{sf} = 10$) increases with decreasing the value of $k_{sf}$ at lower and increases sharply as value of $k_{sf}$ is further decreased beyond 50. Exactly same trend is also followed for lower wall thickness (i.e. $\delta_{sf} = 1$), but at exceedingly lower value of $k_{sf,}$ the value of $Nu_{avg}$ starts decreasing. This is because of no axial conduction in solid wall due to higher axial thermal resistance. At higher wall thickness, the comparative axial thermal resistance will be less. Exactly similar trend is observed when the outlet end is insulated i.e. for the Case-3 heating.
- Overall, higher axial conduction causes the boundary condition experienced at the solid-fluid interface is more towards constant heat flux condition compared to actually applied constant

wall temperature condition on its outer surface.

- Therefore, depending on situation, axial conduction enhance/reduce overall heat transfer process.

## References:


Bahnke G.D., Howard C.P., 1964, The effect of longitudinal heat conduction on periodic-flow heat exchanger performance, Journal Engineering Power 86 (2), pp. 105-120.

Barozzi G.S., Pagliarini G., 1985, A method to solve conjugate heat transfer problems: The case of fully developed laminar flow in a pipe, Journal Heat Mass Transfer 107(1), pp. 77-83.

Celata G.P., Cumo M., Marconi V., McPhail, S.J., and Zummo, G., 2006, Microtube Liquid Single Phase Heat Transfer in Laminar Flow, International Journal Heat Mass Transfer, 49(19–20), pp. 3538–3546.

Cengel, U.A., 2003, Heat Transfer: A Practical Approach, McGraw-Hill, New York, USA.

Chiou J.P., 1980, The advancement of compact heat exchanger theory considering the effects of longitudinal heat conduction and flow non-uniformity. Symposium on compact heat exchangers-history, technological advancement and mechanical design problems. Book no. G00183, HTD Vol. 10, ASME, New York.

Cole K.D., Cetin B., 2011, The effect of axial conduction on heat transfer in a liquid microchannel flow, International Journal Heat Mass Transfer, 54(11–12), pp. 2542–2549.

Cotton M.A., Jackson J.D., 1985, The Effect of heat conduction in a tube wall upon forced convection heat transfer in the thermal entry region. In: Numerical methods in thermal problems, vol IV. Pineridge Press, Swansea, pp. 504–515.

Davis E.J., Gill N.W., 1970, The effect of axial conduction in the wall on heat transfer with laminar flow, International Journal Heat Mass Transfer 13 (3), pp. 459–470.

Faghri M., Sparrow E.M., 1980, Simultaneous wall and fluid axial conduction in laminar pipe-flow heat transfer, Journal Heat Mass Transfer 102 (1), pp. 58-63.

Gamrat G., Marinet M. F., Asendrych D., 2005, Conduction and entrance effects on laminar liquid flow and heat transfer in rectangular microchannels, International Journal Heat Mass Transfer, 48(14), pp. 2943–2954.

García Hernando N., Acosta Iborra A., Ruiz Rivas, U., Izquierdo, M., 2009, Experimental Investigation of fluid flow and heat transfer in a single phase liquid flow micro heat exchanger, International Jornal Heat Mass Transfer 52 (23-24), pp. 5433-5446.

Goodling J.S., 1993, Microchannel heat exchangers: A review, Proc. High Heat Flux Engineering II, July 12-13, San Diego, CA, pp. 66-82.

Hetsroni G., Mosyak A., Pogrebnyak E., Yarin L.P., 2005, Heat transfer in micro channels: comparison of experiments with theory and numerical results, International Journal Heat Mass Transfer, 48(25–26), pp. 5580–5601.

Kakac S., Vasiliev L.L., Bayazitoglu Y., Yener Y., (Eds.) Microscale Heat Transfer: Findamentals and Applications, Springer, Dordrecht, The Netherlands.

Kandlikar, S. G., 2012, History, advances, and challenges in liquid flow and flow boiling heat transfer in microchannels; A critical review, Journal Heat Mass Transfer, 134 034001, pp. 1-15.

Kim S.J., Kim D., 1999, Forced convection in microstructures for electronic equipment cooling, Journal Heat Mass Transfer,121(3), pp. 639–645.

Lelea D., 2007, The conjugate heat transfer of the partially heated micro channels, Heat Mass Transfer, 44(1), pp. 33–41.

Lelea D., 2009, The heat transfer and fluid flow of a partially heated microchannel heat sink, International Community Heat Mass Transfer, 36(8), pp. 794–798.

Maranzana G., Perry I., Maillet D., 2004, Mini- and micro-channels: influence of axial

conduction in the walls. International Journal Heat Mass Transfer, 47(17-18), pp. 3993–4004.

Mehendale S.S, Jacobi A.M., Shah R.K., 2000, Fluid flow and heat transfer at micro and meso scales with application to heat exchanger design, Applied Mech. Rev. 53(7), pp. 175.193.

Moharana M.K., Agarwal G., Khandekar S., 2011, Axial conduction in single-phase simultaneously developing flow in a rectangular mini-channel array, International Journal Thermal Science, 50(6), pp. 1001–1012.

Moharana M.K., Khandekar S., 2012, Numerical study of axial back conduction in microtubes, Proceedings of the Thirty Ninth National Conference on Fluid Mechanics and Fluid Power, December 13-15, SVNIT Surat, Gujarat, India.

Moharana M.K., Khandekar S., 2012, Effect of channel shape on axial back conduction in the solid substrate of microchannels, Proceedings of the 3rd European Conference on Microfluidics - Microfluidics, December 3-5, Heidelberg, Germany.

Moharana M.K., Singh P.K., Khandekar S., 2012, Optimum Nusselt number for simultaneously developing internal flow under conjugate conditions in a square microchannel, Journal Heat Mass Transfer, (134) 071703, pp. 01-10.

Moore G.E., 1998, Cramming more components onto integrated circuits, Electronics, proceedings of the IEEE, 86, pp. 82-85.

Mori S., Sakakibara M., Tanimoto A., 1974, Steady state heat transfer to laminar flow in circular tube with conduction in the tube wall, Heat Transfer Japanese Research, 3(2), pp. 37-46.

Mori S., Kawamura Y., Tanimoto A., 1979, Conjugated heat transfer to laminar flow with internal heat source in a parallel plate channel, Canadian J. Chem. Eng. 57(6), pp. 698 - 703.

Morini, G. L., 2006, Scaling effects for liquid flows in microchannels, Heat Transfer Engineering, 27(4), pp. 64–73.

Peterson R.B., 1999, Numerical modeling of conduction effects in microscale counter flow heat exchangers, Microscale Thermophysics Engineering 3(1), pp. 17-30.

Petukhov B.S., 1967, .Heat transfer and drag of laminar flow of liquid in pipes. Energiya, Moscow

Qu W., Mala G.M., Li D., 2000, Heat transfer for water flow in trapezoidal silicon microchannels, International Journal Heat Mass Transfer 43, pp. 3925-3936.

Rahimi M., Mehryar R., 2012, Numerical study of axial heat conduction effects on the local Nusselt number at the entrance and ending regions of a circular microchannel, International Journal Thermal Sciences, 59, pp. 87-94

Rosa P., Karayiannis T.G., Collins M.W., 2009, Single-phase heat transfer in microchannels: The importance of scaling effects, Applied Thermal Engineering 29(17-18), pp. 3447–3468

Satapathy A. K., 2010, Slip flow heat transfer in a semi-infinite microchannel with axial conduction, Journal of Mechanical Engineering Science, 224(2), pp. 357-361.

Tiselj I., Hetsroni G., Mavko B., Mosyak A., Pogrebnyak E., Segal Z., 2004, Effect of axial conduction on the heat transfer in micro-channels., International journal heat mass transfer 47, pp. 2551–2565.

Toh K.C., Chen X.Y., Chai J.C., 2002, Numerical computation of fluid flow and heat transfer in microchannels, International Journal Heat Mass Transfer 45(26), pp. 5133–5141.

Tuckerman D.B., Pease R.F.W., 1981, High-performance heat sinking for VLSI, IEEE Electron Device Letters, 2(5), pp. 126–129.

Yang C.Y., Lin T.Y., 2007, Heat transfer characteristics of water flow in microtubes, Exp. Thermal Fluid Science 32 (2), pp. 432-439.

Yarin, L. P., Mosyak, A., and Hetsroni, G., 2009, Fluid Flow, Heat Transfer and Boiling in

Micro-Channels, Springer-Verlag, Berlin.

Zhang S.X., He Y.L., Lauriat, G., Tao, W.Q., 2010, Numerical studies of simultaneously developing laminar flow and heat transfer in microtubes with thick wall and constant outside wall temperature,"International Journal Heat Mass Transfer, 53(19–20), pp. 3977–3989.